

POLYMERIZATION AND CHARACTERIZATION OF  
ALLYL METHACRYLATE

A THESIS SUBMITTED TO  
THE GRADUATE SCHOOL OF NATURAL AND APPLIED SCIENCES  
OF  
MIDDLE EAST TECHNICAL UNIVERSITY

BY

TUĞBA VARDARELİ

IN PARTIAL FULFILLMENT OF THE REQUIREMENTS  
FOR  
THE DEGREE OF MASTER OF SCIENCE  
IN  
POLYMER SCIENCE AND TECHNOLOGY

AUGUST 2006

Approval of the Graduates School of Natural and Applied Sciences

\_\_\_\_\_  
Prof. Dr. Canan ÖZGEN  
Director

I certify that this thesis satisfies all the requirements as a thesis for the degree of Master of Science in Polymer Science and Technology.

\_\_\_\_\_  
Assoc.Prof.Dr.Göknur BAYRAM  
Head of Department

This is to certify that we have read this thesis and that in our opinion it is fully adequate, in scope and quality, as a thesis for the degree of Master of Science in Polymer Science and Technology.

\_\_\_\_\_  
Prof. Dr. Ali USANMAZ  
(Supervisor)

Examining Committee in Charge

Prof. Dr. Oya ŞANLI (GAZİ, CHEM) \_\_\_\_\_

Prof. Dr. Ali USANMAZ (METU, PST) \_\_\_\_\_

Prof. Dr. Levent TOPPARE (METU, CHEM) \_\_\_\_\_

Assist. Prof. Dr. Ayşen YILMAZ (METU, CHEM) \_\_\_\_\_

Assoc. Prof. Dr. H. Nur TESTERECİ (KIRIKKALE, CHEM) \_\_\_\_\_

**I hereby declare that all information in this document has been obtained and presented in accordance with academic rules and ethical conduct. I also declare that, as required by these rules and conduct, I have fully cited and referenced all material and results that are not original to this work.**

Name, Last name :

Signature :

## **ABSTRACT**

### POLYMERIZATION AND CHARACTERIZATION OF ALLYL METHACRYLATE

VARDARELİ, Tuğba

M.Sc., Department of Polymer Science and Technology

Supervisor : Prof. Dr. Ali USANMAZ

August 2006, 83 pages

Allyl methacrylate, AMA was polymerized by chemical initiator and by  $\gamma$ -radiation under different conditions. The polymer obtained is mostly gel type with some soluble fractions at lower conversions. Arrhenius activation energy is 82.3 kJ/mol for chemical initiated polymerization. The polymer was characterized by FT-IR, NMR, DSC, TGA, XPS, XRD, DLS, and MS methods. It was found that about 98-99% of allyl side groups retained as pendant even after completion of the polymerization, while 1-2% may give crosslinking and/or cyclization that yields lactones and anhydrides. The spectroscopic and thermal results of the work showed that the reaction is not cyclopolymerization, but may have end group cyclization. Molecular weight of  $1.1 \times 10^6$  was measured by DLS. Therefore, insolubility is due to the high molecular weight of polymer,

even in the early stage of polymerization rather than crosslinking. The T<sub>g</sub> of PAMA was observed as 94°C before curing, upon curing at 150-200°C, T<sub>g</sub> increased to 211°C as measured by DSC. The thermal treatment of polymer at about 350°C gave anhydride by linkage type degradation, following side group cyclization. The XPS analysis showed the presence of radical fragments of AIBN and CCl<sub>4</sub> associated with oligomers. The MS and TGA thermograms showed two or three stage degradations depending on solubility. The first stage was mostly linkage type degradation for the fragmentation of pendant allyl groups at 225-350°C. In the second stage, at 395-515°C, the degradation is random scission and depolymerization.

Keywords: allyl methacrylate, degradation, X-Ray Photoelectron Spectroscopy (XPS), Mass Spectroscopy (MS), Thermal Gravimetric Analysis (TGA)

# ÖZ

## ALİL METAKRİLATIN POLİMERİZASYONU VE POLİMER KARAKTERİZASYONU

VARDARELİ, Tuğba

Y.L., Polimer Bilimi ve Teknolojisi Bölümü  
Danışman : Prof. Dr. Ali USANMAZ

Ağustos 2006, 83 sayfa

Alil metakrilat, AMA farklı koşullarda kimyasal başlatıcı ve  $\gamma$ -ışınları kullanılarak polimerleştirilmiştir. Elde edilen polimer, genellikle bilinen çözücülerde çözünmeyen jel tipindedir. Kimyasal başlatıcılarla başlatılan polimerleşmede Arrhenius aktivasyon enerjisi 82.3 kJ/mol olarak hesaplanmıştır. Polimer FT-IR, NMR, DSC, TGA, XPS, XRD, DLS, ve MS metodları ile karakterize edilmiştir. Alil yan gruplarının %98-99'u polimerizasyon bittikten sonra yerlerini korurken, %1-2'si çapraz bağlanma ve/veya halka reaksiyonu ile lakton oluştuşlardır. Spektroskopik ve ısasal sonuçlar, polimerizasyonun halka polimerizasyonu olmadığını, fakat son grup halka polimerleşmesi olabileceğini göstermektedir. DLS 'de moleköl ağırlığı  $1.1 \times 10^6$  olarak ölçülmüştür. Polimerin çözünmez olması çapraz

bařlanmadan ok yksek molekl aęırlıęından kaynaklanmaktadır. Polimerin DSC 'de gzlenen Tg 'si 94°C' dir. Ancak 150-200°C' de yařlandırmadan sonra Tg 211°C' ye ykselmiřtir. Polimer 350°C' de yapılan ısısal iřlemden sonra yan-baęlantı tipi bozunma ve bunu izleyen yan grup halka reaksiyonu sonucu lakton ve/veya anhidrit vermiřtir. XPS analizi AIBN ve CCl<sub>4</sub> radikal gruplarının oligomerlerde bulunduęunu gstermektedir. MS ve TGA termogramları polimerin znrlęne baęlı olarak iki veya  ařamada bozunduęunu gstermektedir. Birinci ařamada, 225-350°C, alil grupları yan-baęlantı tipi bozunmaktadır. İkinci ařamada ise, 395-515°C, rastgele blnme ve depolimerizasyon tipi bozunma oluřmaktadır.

Anahtar Kelimeler: alil metakrilat, bozunma, X-iřin fotoelektron spektroskopisi (XFS), Ktle Spectrometresi (MS), Thermogravimetrik Analiz (TGA)

*To the memory of my father,*

## **ACKNOWLEDGEMENTS**

I would like to thank my supervisor, Prof. Dr. Ali Usanmaz, for his great guidance and continuous support in my M.Sc. program. I am very honored to be his student. He taught me how to conduct research and write academic papers.

Thanks also to my Lab mates Elif Vargün, Bengi Aran, Elif Anaçođlu, Selda Keskin for their friendship, understanding and being so helpful any times of need. Thanks to Central Laboratory staff for their valuable helps during the experiments.

Also thanks to my family; my mother and my father. The happy memory of my father still provides a persistent inspiration for my journey in this life. I know you watch me at all times and proud of me.

Lastly, thanks to my husband, Fatih Vardareli for his constant support and patience during the M.Sc. period. Without his encouragement and love, I could not have finished my M.Sc. program. You know you are the one.

## TABLE OF CONTENTS

<b>PLAGIARISM.....</b>	<b>iii</b>
<b>ABSTRACT.....</b>	<b>iv</b>
<b>ÖZ .....</b>	<b>vi</b>
<b>ACKNOWLEDGEMENTS.....</b>	<b>ix</b>
<b>TABLE OF CONTENTS.....</b>	<b>x</b>
<b>LIST OF TABLES.....</b>	<b>xiii</b>
<b>LIST OF FIGURES .....</b>	<b>xiv</b>
<b>CHAPTERS .....</b>	<b>1</b>
1. INTRODUCTION.....	1
1.1. ALLYL METHACRYLATE.....	1
1.2. FREE RADICAL POLYMERIZATION.....	2
1.2.1. Initiation .....	2
1.2.2. Propagation.....	4
1.2.3. Termination.....	5
1.3. ATOM TRANSFER RADICAL POLYMERIZATION (ATRP) .....	8
1.4. DEGRADATION.....	10
1.5. XPS (ESCA).....	12
1.6. POLYMERIZATION OF AMA .....	15
1.7. AIM OF THIS STUDY .....	18

2. EXPERIMENTAL.....	19
2.1. MATERIALS.....	19
2.1.1. Monomer .....	19
2.1.2. Ligand .....	19
2.1.3. Catalyst .....	20
2.1.4. Initiator.....	20
2.1.5. Solvents.....	21
2.2. INSTRUMENTATION.....	21
2.2.1. Polymerization Tubes.....	21
2.2.2. High Vacuum System.....	22
2.2.3. <sup>60</sup> Co γ-Ray Source .....	22
2.2.4. Infrared Spectrometer (FT-IR).....	22
2.2.5. Nuclear Magnetic Resonance (NMR) .....	22
2.2.6. Differential Scanning Calorimeter (DSC).....	23
2.2.7. Thermal Gravimetric Analysis (TGA-FT-IR) .....	23
2.2.8. Mass Spectrometer (MS).....	23
2.2.9. X-Ray Photoelectron Spectroscopy (XPS).....	23
2.2.10. Dynamic Light Scattering (DLS) .....	24
2.2.11. Refractometer .....	24
2.2.12. X-Ray Powder Diffractometer (XRD).....	24
2.3. EXPERIMENTAL PROCEDURE .....	24
2.3.1. Bulk Polymerization of AMA via Chemical Initiation in the Presence of Atmospheric Oxygen .....	24
2.3.2. Solution Polymerization of AMA via Chemical Initiation under Vacuum.....	25
2.3.3. Radiation Induced Bulk Polymerization of AMA in the presence of Atmospheric Oxygen .....	25
2.3.4. Radiation Induced Solution Polymerization of AMA under Vacuum.....	26

2.3.5. Radiation Induced Atom Transfer Radical Polymerization of AMA under Vacuum.....	26
3. RESULTS AND DISCUSSION .....	27
3.1. <i>POLYMERIZATION OF AMA</i> .....	27
3.1.1. Polymerization of AMA via Chemical Initiation.....	27
3.1.2. Radiation Induced Polymerization of AMA .....	33
3.1.3. Arrhenius Activation Energy for Chemically Initiated Polymerization of AMA.....	37
3.2. <i>CHARACTERIZATION OF PAMA</i> .....	40
3.2.1. FT-IR Investigation.....	40
3.2.2. NMR Investigation .....	46
3.2.3. DSC Investigation.....	54
3.2.4. TGA Investigation.....	56
3.2.5. MS Investigation.....	61
3.2.6. XPS Investigation .....	73
3.2.7. DLS Investigation .....	78
3.2.8. Powder XRD Investigation.....	79
4. CONCLUSION.....	80
<b>REFERENCES.....</b>	<b>82</b>

## LIST OF TABLES

<b>Table 1.1</b> Physical Properties of AMA .....	2
<b>Table 3.1</b> Bulk polymerization of AMA by BPO in the presence of atmospheric oxygen at 70°C.....	28
<b>Table 3.2</b> Solution polymerization of AMA by AIBN at 50°C .....	30
<b>Table 3.3</b> Solution polymerization of AMA by AIBN at 60°C .....	31
<b>Table 3.4</b> Solution polymerization of AMA by AIBN at 70°C .....	32
<b>Table 3.5</b> Radiation induced bulk polymerization of AMA in the presence of atmospheric oxygen .....	34
<b>Table 3.6</b> Radiation induced solution polymerization of AMA under vacuum .....	35
<b>Table 3.7</b> Radiation induced atom transfer radical polymerization of AMA under vacuum.....	36
<b>Table 3.8</b> Reaction rate constants for solution polymerization of AMA ...	39
<b>Table 3.9</b> The peak assignments for the FT-IR spectrum of AMA and PAMA .....	40
<b>Table 3.10</b> <sup>1</sup> H-NMR spectrum of AMA and PAMA .....	46
<b>Table 3.11</b> <sup>13</sup> C-NMR spectrum of AMA .....	50
<b>Table 3.12</b> The relative abundances of the peaks and their fragments from insoluble PAMA fraction .....	66
<b>Table 3.13</b> The relative abundances of the peaks and their fragments from soluble PAMA fraction.....	71
<b>Table 3.14</b> The assignment of atomic eV to XPS peaks for PAMA.....	74
<b>Table 3.15</b> DLS results for soluble fraction of PAMA.....	78

## LIST OF FIGURES

<b>Figure 3.1</b> Polymerization of AMA (a) in bulk by BPO in the presence of atmospheric oxygen at 70°C and in CCl <sub>4</sub> by AIBN at (b) 50, (c) 60, and (d) 70°C.....	29
<b>Figure 3.2</b> The percent conversion (a) total and (b) insoluble fraction in toluene against time at 50°C .....	33
<b>Figure 3.3</b> Radiation induced polymerization of AMA (a) in bulk in the presence of atmospheric oxygen, (b) in CCl <sub>4</sub> solution under vacuum, and (c) ATRP under vacuum.....	34
<b>Figure 3.4</b> The plots of $\ln[M]/[M_0]$ vs. time for solution polymerization at (a) 50, (b) 60, and (c) 70°C .....	38
<b>Figure 3.5</b> $\ln k$ vs $1/T$ .....	39
<b>Figure 3.6</b> FT-IR spectra of (a) AMA, (b) PAMA from bulk polymerization by BPO in the presence of atmospheric oxygen (80.7%) .....	43
<b>Figure 3.7</b> FT-IR spectra of (a) AMA and soluble PAMA fraction from solution polymerization by AIBN under vacuum with a conversion of (b) 10%, (c) 45%, (d) 79% .....	44
<b>Figure 3.8</b> FT-IR spectra of residual PAMA pretreated at (a) 280 and (b) 350°C.....	45
<b>Figure 3.9</b> <sup>1</sup> H-NMR spectra of (a) AMA, (b) PAMA from ATRP under vacuum (58.83%) .....	48
<b>Figure 3.10</b> <sup>1</sup> H-NMR spectrum of soluble PAMA fraction from solution polymerization by AIBN under vacuum at 50°C (44.92%) .....	49

<b>Figure 3.11</b> $^{13}\text{C}$ -NMR of (a) AMA and (b) PAMA from radiation induced solution polymerization under vacuum (99.81%).....	52
<b>Figure 3.12</b> $^{13}\text{C}$ -NMR of (a) soluble PAMA fraction from solution polymerization by AIBN under vacuum at 50°C (44.92%) and (b) residual PAMA after pyrolysis at 350°C.....	53
<b>Figure 3.13</b> DSC thermograms of PAMA (a) first run and (b) second run from radiation induced polymerization under vacuum (93.68%).....	55
<b>Figure 3.14</b> DSC thermograms of soluble fraction of PAMA (a) first run and (b) second run from solution polymerization under vacuum at 50°C (71.36%).....	55
<b>Figure 3.15</b> TGA thermogram of insoluble PAMA fraction from solution polymerization by AIBN at 50°C (67.87%) .....	58
<b>Figure 3.16</b> FT-IR spectra of TGA degradation fragments of PAMA at (a) 271, (b) 343, (c) 402, and (d) 417°C.....	58
<b>Figure 3.17</b> TGA thermogram of soluble PAMA from solution polymerization by AIBN at 50°C (67.66%) .....	60
<b>Figure 3.18</b> FT-IR spectra of TGA degradation fragments of PAMA at (a) 225, (b) 387, and (c) 579°C.....	60
<b>Figure 3.19</b> Mass thermograms of (a) insoluble and (b) soluble PAMA fraction.....	61
<b>Figure 3.20</b> Fragments from insoluble PAMA fraction obtained at 142°C	64
<b>Figure 3.21</b> Fragments from insoluble PAMA fraction obtained at 335°C	64
<b>Figure 3.22</b> Fragments from insoluble PAMA fraction obtained at 442°C	65
<b>Figure 3.23</b> Fragments from soluble PAMA fraction obtained at 309°C..	69
<b>Figure 3.24</b> Fragments from soluble PAMA fraction obtained at 405°C..	69
<b>Figure 3.25</b> Fragments from soluble PAMA fraction obtained at 441°C..	70
<b>Figure 3.26</b> XPS spectra of PAMA (a) before, (b) after pyrolysis at 350°C .....	76
<b>Figure 3.27</b> XPS spectra of peak fitting of (a) C 1s and (b) O 1s of PAMA .....	77

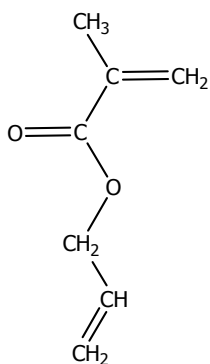
**Figure 3.28** XRD patterns of (a) PAMA with 62% conversion, (b) same PAMA cured at 125°C, (c) cured at 175°C , and (d) extended form of (c)  
.....79

# CHAPTER 1

## 1. INTRODUCTION

### 1.1. ALLYL METHACRYLATE

Allyl methacrylate, AMA is a difunctional monomer containing two unsaturated reactive sites with the following structure:



allyl methacrylate

AMA is a clear, colorless liquid with a pungent odor. It is toxic and flammable. It can polymerize by sunlight and/or heat, therefore is inhibited with 50 to 185 ppm monomethyl ether hydroquinone (MEHQ). The physical properties of AMA are given in Table 1.1.

**Table 1.1** Physical Properties of AMA

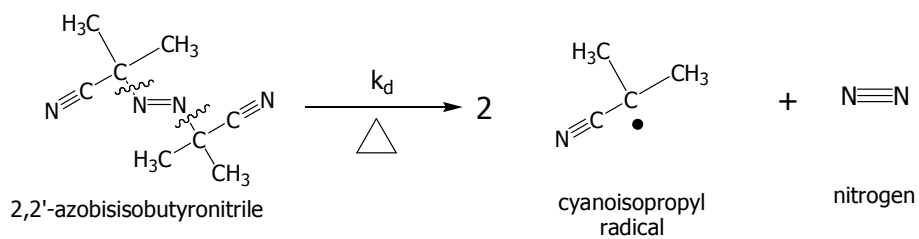
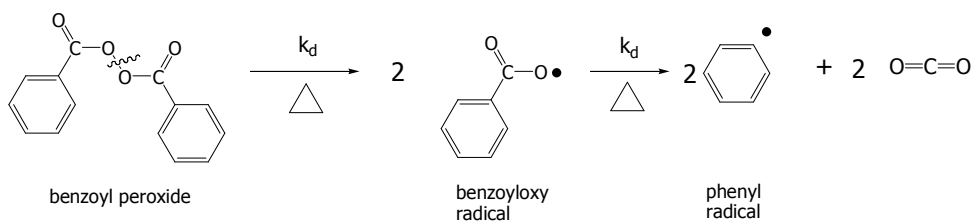
Property	Value
Boiling Point, (°C @ 760mmHg)	140
Freezing Point, (°C @ 760mmHg)	-65
Flash Point, (°C)	35
Density, g/mL (@ 20 °C)	0.945

## 1.2. FREE RADICAL POLYMERIZATION

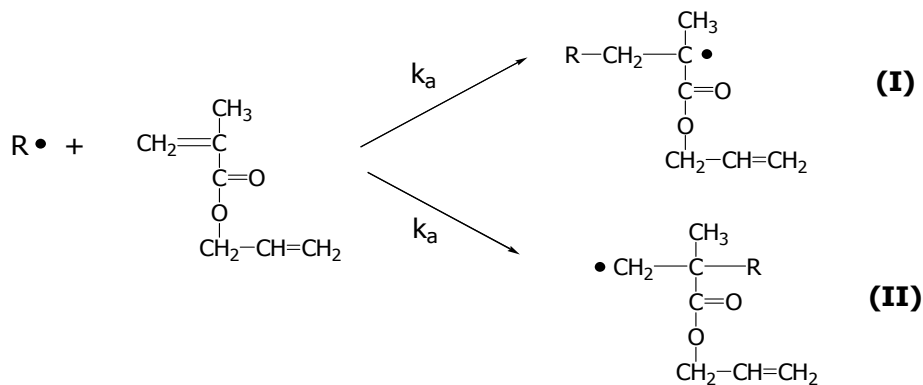
Free radical polymerization is the most important chain polymerization which is initiated by a free radical. It consists of initiation, propagation, and termination steps.

### 1.2.1. Initiation

In the initiation step, first the initiator(I) dissociates to radical (R·) as follows:



The second step of initiation is the addition of radical ( $R\cdot$ ) to monomer molecule ( $M$ ) to form  $RM\cdot$ . The addition of monomer to a free radical can take place in either of two ways as follows:



Radical (I) can be stabilized by the resonance effects of the substituents. Radical (I) is less sterically hindered compared to radical (II) because attack at the methylene carbon is easier. Therefore, radical (I) is favored.

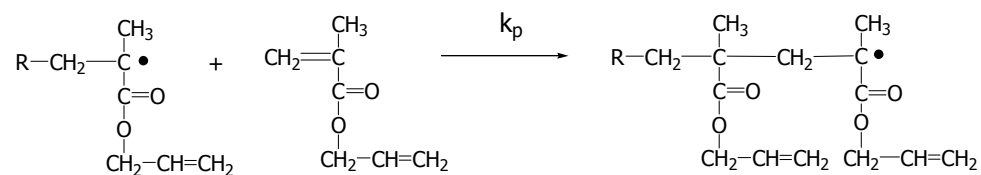
The rate determining step is the dissociation of the initiator and the rate of initiation is given by

$$R_i = 2fk_d[I] = d[R\bullet] / dt \dots\dots\dots(1.2.1)$$

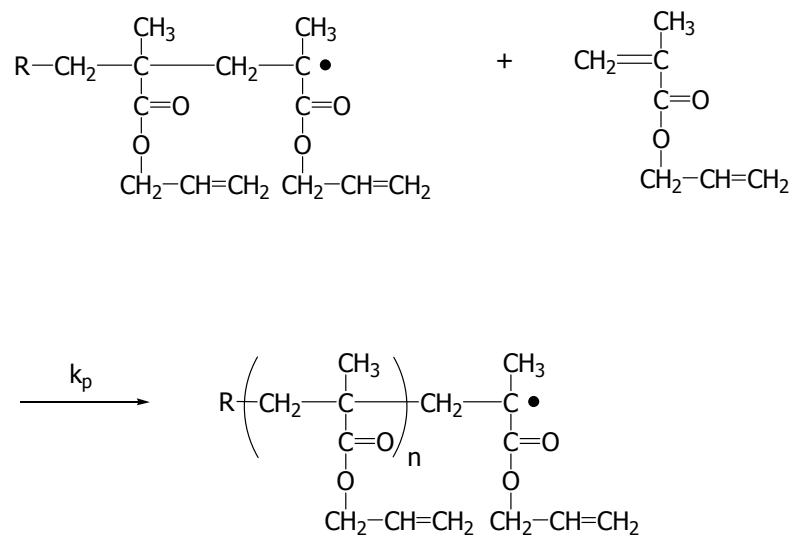
where  $k_d$  is the dissociation rate constant,  $[I]$  is the concentration of the initiator, and  $f$  is the initiator efficiency.

### 1.2.2. Propagation

In the propagation step, more monomer units are added as follows:



Monomers are added sequentially during subsequent propagation steps and newly formed radical has the same reactivity.



The rate of propagation is represented as

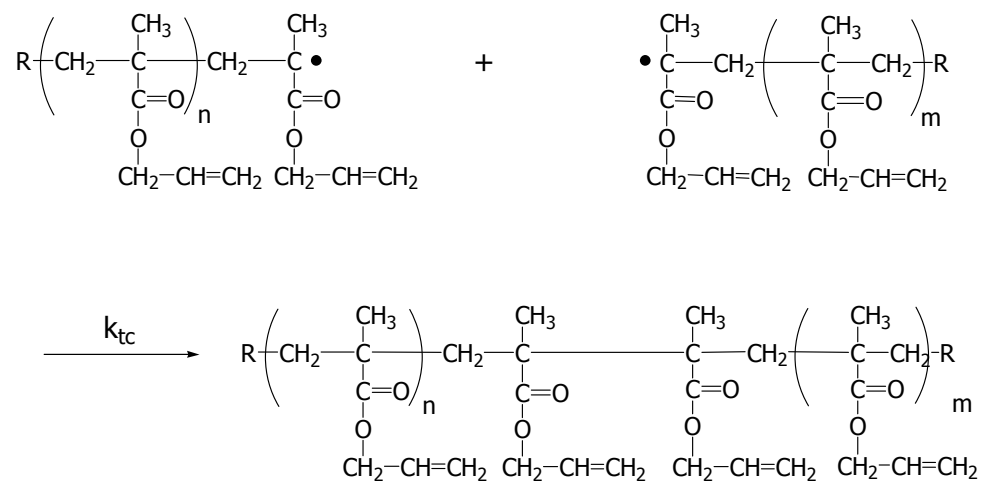
$$R_p = k_p [M\cdot] [M] = -d[M] / dt \quad (1.2.2)$$

where  $k_p$  is the propagation rate constant.

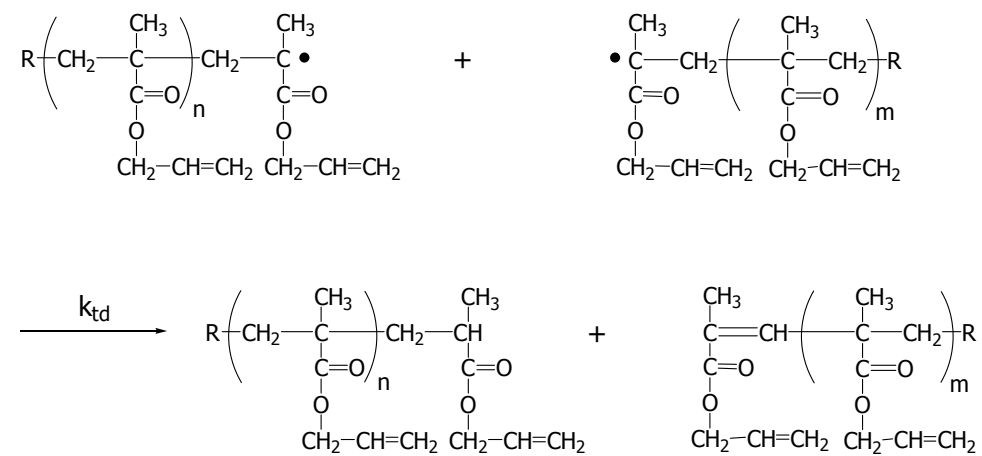
### 1.2.3. Termination

The termination step occurs by combination and disproportionation of bimolecular reaction and represented as follows:

Combination:



Disproportionation:



The overall rate of termination is given by

$$R_t = 2 k_{tc} [M\bullet][M\bullet] + 2 k_{td} [M\bullet][M\bullet] = 2 k_t [M\bullet]^2 \quad (1.2.3)$$

where  $k_t$  is the overall rate constant for termination and is given by

$$k_t = k_{tc} + k_{td}$$

At steady-state conditions rate of initiation and termination are equal

$$2fk_d [I] = 2 k_t [M\bullet]^2$$

So the steady state total concentration of all radical species is given by

$$[M\bullet] = (fk_d [I] / k_t)^{1/2} \quad (1.2.4)$$

Substituting (1.2.4) into (1.2.2) will give general rate expression

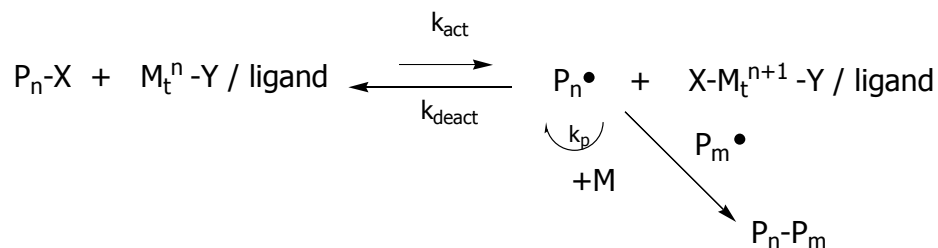
$$R_p = -d[M] / dt = k_p [M] [I]^{1/2} (fk_d / k_t)^{1/2} \dots\dots\dots(1.2.5)$$

The integration will be as follows:

$$\ln [M / M_0] = -k [I]^{1/2} t = -k' t \dots\dots\dots(1.2.6)$$

### 1.3. ATOM TRANSFER RADICAL POLYMERIZATION (ATRP)

In ATRP, the transition metal complex ( $M_t^{n+1}-Y/L$ ) is formed by the combination of  $M_t^n$ , which is the transition metal catalyst in the lower oxidation state,  $n$ , with appropriate ligand(s),  $L$ . The radicals are generated through a reversible redox process catalyzed by a transition metal complex which undergoes one electron oxidation with the abstraction of a halogen atom,  $X$ , from the initiator molecule,  $R-X$ , generating an oxidized transition metal halide complex ( $X-M_t^{n+1}-Y/L$ ). This process occurs with a rate constant of activation,  $k_{act}$ , and deactivation  $k_{deact}$ , represented as

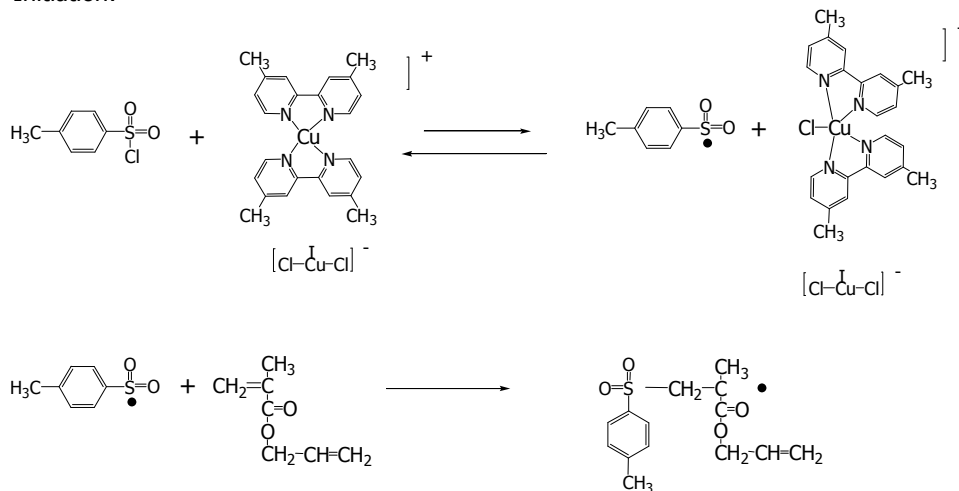


The rate expression is

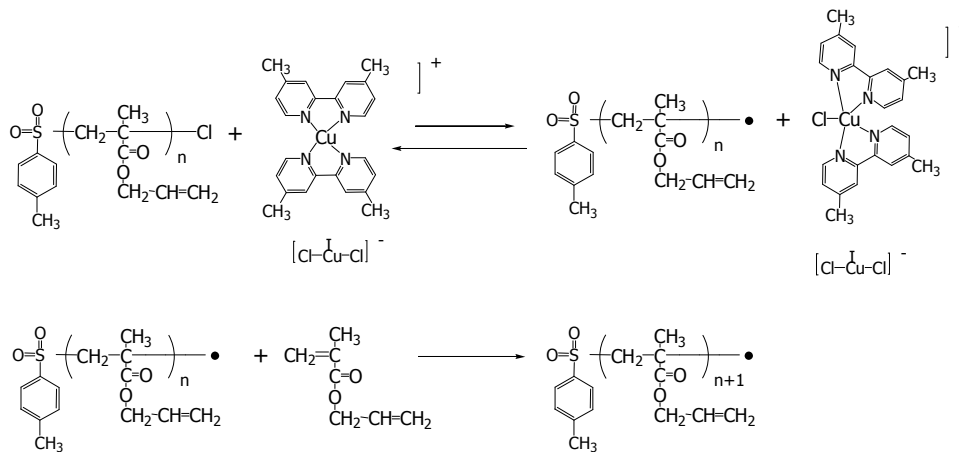
$$R_p = k_{act} / k_{deact} = [P_n^\bullet] [Cu^{II}Cl_2] / [P_n-X] [Cu^I Cl]$$

The polymerization mechanism of AMA by ATRP method is given as

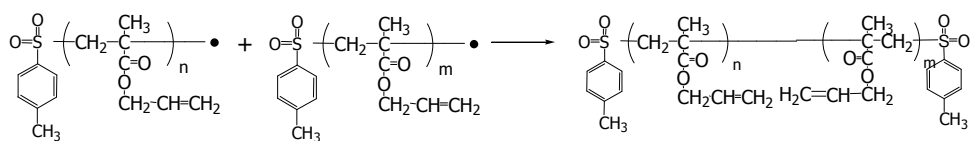
Initiation:



Propagation:



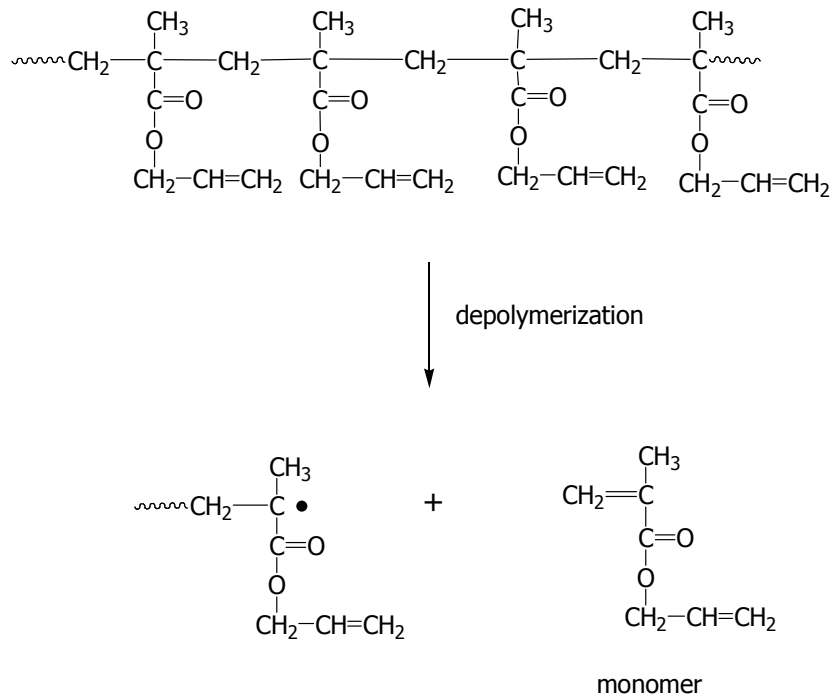
Termination:



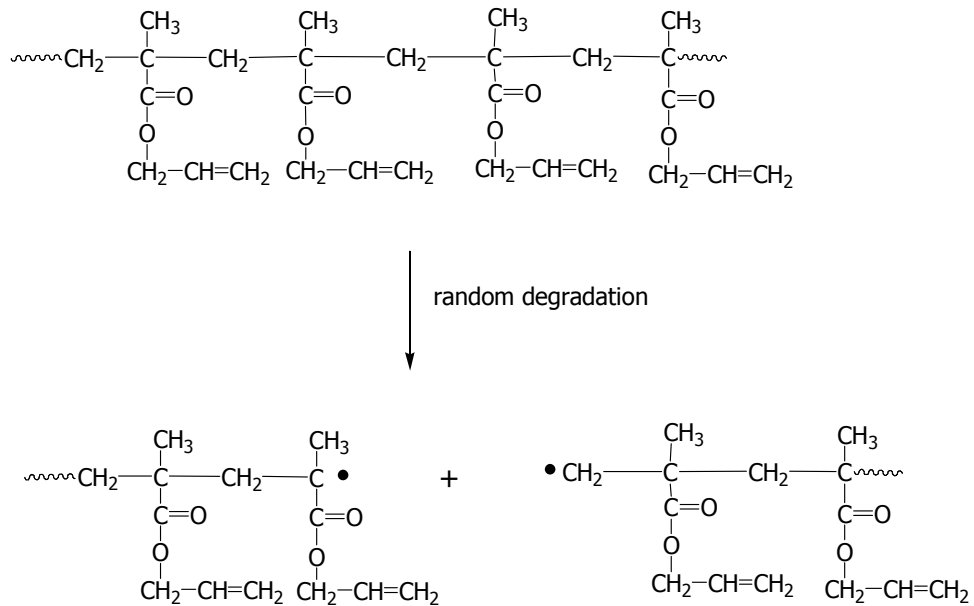
## 1.4. DEGRADATION

The thermal stability of a polymer depends on its bonding energies. There are three types of polymer degradation processes;

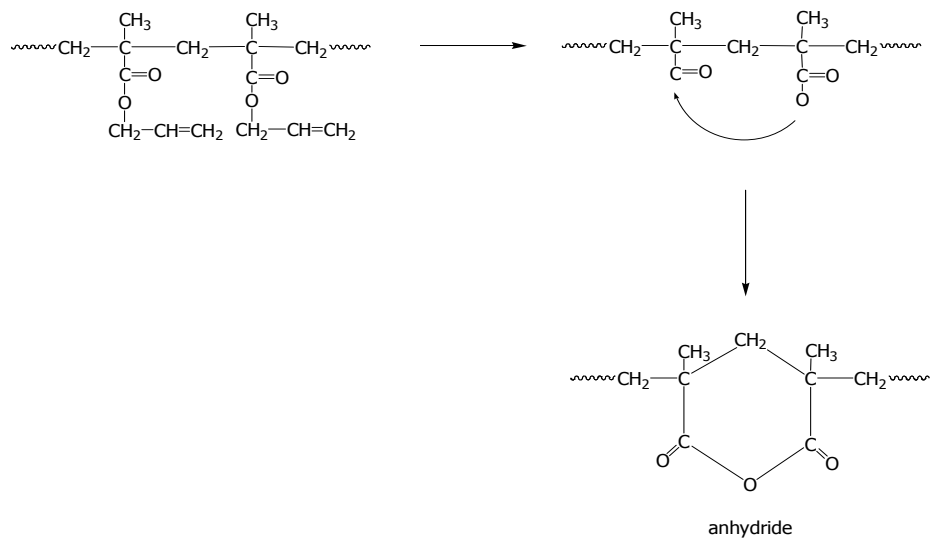
(i) Chain depolymerization (unzipping or depropagation) involves the successive release of monomer units from a chain end.



(ii) Random degradation, chain rupture or scission occurs at random points along the chain, resulting with different length of polymer segments and/or oligomers.



(iii) Linkage degradation (side group degradation): The side group of polymer chain is degraded with involvement of gas molecules or resulting with side group cyclization (e.g anhydride and/or lactones formation).



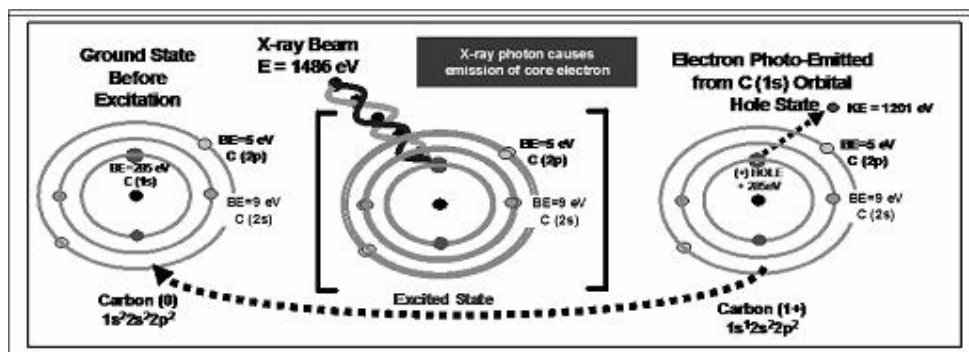
These three types of degradation can occur separately or in combination depending on the degradation conditions (e.g temperature).

### 1.5. XPS (ESCA)

X-Ray Photoelectron Spectroscopy (XPS) is a general type of X-Ray Scattering Spectroscopy for the soft radiation. Electron Spectroscopy for Chemical Analysis (ESCA) is a surface chemical analysis technique of XPS. The method can be qualitative and quantitative within the surface of a material (0.5-10nm).

XPS was developed in the mid-1960's by Kai Siegbahn and his coworkers at the university of Uppsala, Sweden. This technique is based on the photoelectric effect. Each atom on the surface has core electron with the characteristic binding energy (BE) that is conceptually equal to the ionization energy of that electron. When an X-Ray beam directs to the

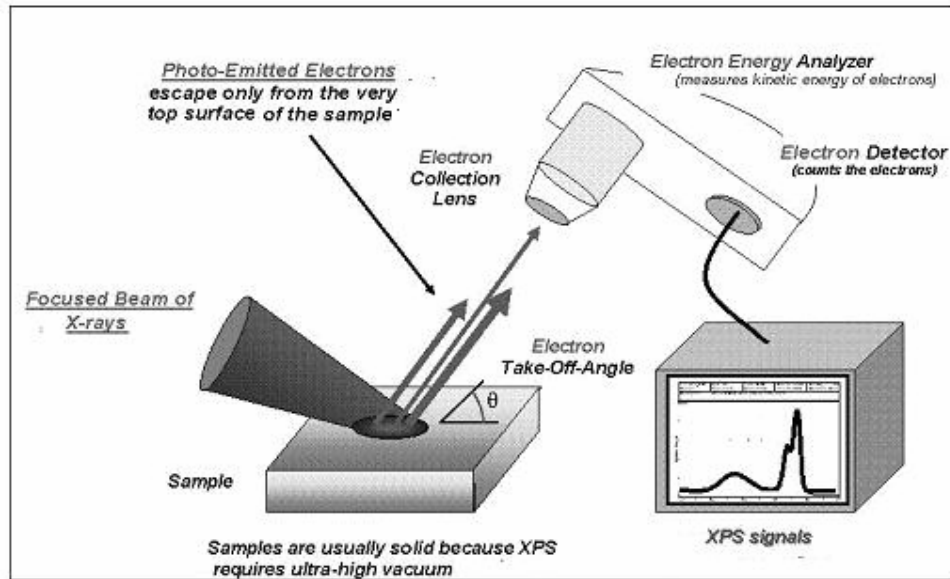
sample surface, the energy of the X-Ray photon is absorbed by the core electron of the atom in a molecule. If the photon energy,  $h\nu$ , is large enough, the core electron will then be broken away from the atom, as shown below:



The emitted electron with the kinetic energy  $KE$  is referred to as photoelectron. The binding energy of the core electron is given by

$$E_b = h\nu - E_k - \Phi$$

where  $h\nu$  is the X-Ray photon energy (for monochromatic  $AlK\alpha$ ,  $h\nu = 1486.6$  eV, for non-chromatic  $MgK\alpha$   $h\nu = 1253$  eV),  $E_k$  is the kinetic energy of the photoelectron, which can be measured by the energy analyzer, and  $\Phi$  is the work function induced by the analyzer, about 4-5 eV,  $h$  is the Planck's constant ( $6.63 \times 10^{-34}$  J.s) and  $\nu$  is the frequency (Hz) of the radiation. A typical XPS instrument is shown below:



To count the number of electrons at each KE value, with a minimum error, XPS must be performed under ultra-high vacuum (UHV- $10^{-8}$ - $10^{-9}$  mbar) conditions since electron counting detectors in XPS instruments are typically one meter away from the material irradiated with X-rays.

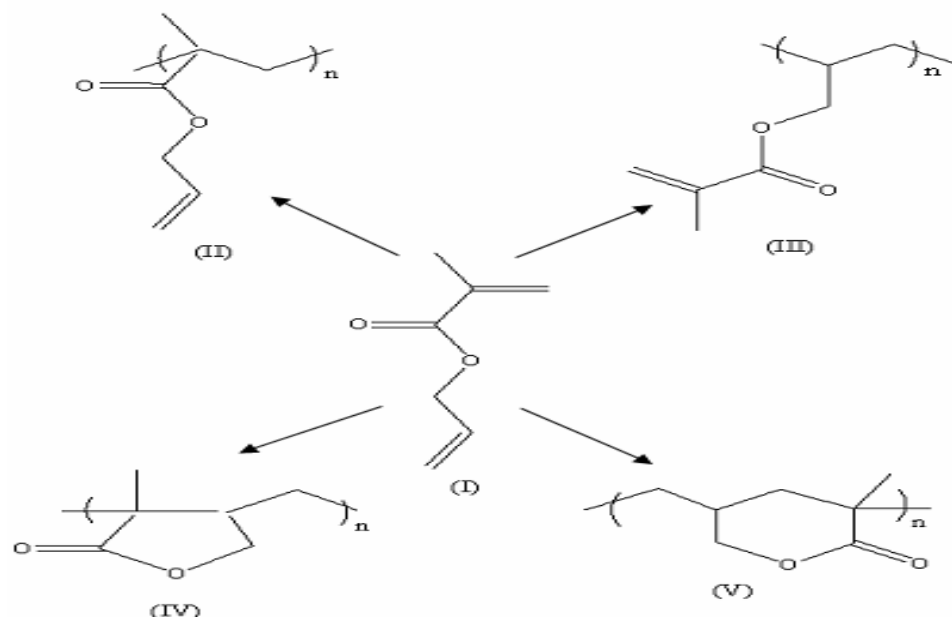
In most cases the binding energies of the core electronic levels are uniquely different for each specific element, which seems like a "fingerprint". Thus, almost all elements except hydrogen up to beryllium can be detected by measuring the binding energies of its core electron. Furthermore, the binding energy of core electron is very sensitive to the chemical environment of the element. The same atom is bonded to different chemical species, leading to the change in the binding energy of its core electron. The variation of binding energy results in the shift of the corresponding XPS peak, ranging from 0.1eV to 10eV. This effect is

termed as a "chemical shift", which can be applied to studying the chemical status of element in the surface.

A typical XPS spectrum is a plot of the number of electrons detected (Y-axis) versus the binding energy of the electrons detected (X-axis). Each element produces a characteristic set of XPS peaks at characteristic binding energy values that directly identify each element that exists in or on the surface of the material being analyzed. These characteristic peaks correspond to the electron configuration of the electrons within the atoms, e.g., 1s, 2s, 2p, 3s, etc. The number of detected electrons in each of the characteristic peaks is directly related to the amount of element within the area irradiated. To generate atomic percentage values, each raw XPS signal must be corrected by dividing its signal intensity (number of electrons detected) by a "relative sensitivity factor" (RSF) and normalized over all of the elements detected.

## 1.6. POLYMERIZATION OF AMA

Allyl methacrylate, AMA (I) is a difunctional monomer with vinyl and allyl groups with different reactivities. The polymerization can be carried out on either of these two unsaturated groups as well as cyclization giving five- and/or six-membered lactone rings.



Allyl methacrylate, AMA was polymerized for the first time in 1946<sup>1</sup>. Since then, polymerization of AMA have been reported by different techniques<sup>1-17</sup>. Anionic polymerization<sup>2,3</sup> of AMA gives linear polymer soluble in most solvents. This type of polymerization was shown<sup>3</sup> to progress through vinyl groups giving poly(allyl methacrylate), PAMA (II), which has a molecular weight up to  $1-2 \times 10^4$ . They also suggested that the anionic initiator is effective for the vinyl groups, without responding to allyl groups. However, this argument is not supported by further experimental results since the linear polymer is insoluble when the molecular weight is high. Most of the reported free radical polymerization<sup>4-11</sup> of AMA give insoluble gel type polymers. However, Higgins and Weale<sup>5</sup> obtained soluble polymers when free radical polymerization was carried out in solution. They suggested the formation of five- and/or six-membered lactone rings by cyclopolymerization based on the IR spectrum. They also pointed out that the solvent molecules

terminated the allyl radical preventing crosslinking and making the polymer soluble. Free radical polymerization in bulk mostly gives crosslinking and/or cyclization (IV-V). Even though the cyclopolymerization is not definitely shown by experimental results, Matsumoto et al<sup>6</sup> claimed that the crosslinking is due to cyclopolymerization that gives lactones. However, this is contradicted by NMR results. Heatley et al<sup>7</sup> pointed the same issue when characterizing the polymer obtained by free radical homo and copolymerization of AMA using NMR. Matsumoto<sup>8,9,10</sup> reported in his later works that the gel formation was due to the crosslinking and calculated the degree of crosslinking theoretically. Hirano et al<sup>12</sup> studied stereoregularity of oligo(AMA) by <sup>13</sup>C-NMR and showed the heterotactic nature of the polymer chain. The polymerization of AMA by ATRP method<sup>11,13,14</sup> was reported to give the polymer (type (II)) with molecular weight smaller than  $2 \times 10^4$  which was also reported for anionic polymerization<sup>2,3</sup> with polydispersity index (Pd) close to one<sup>13</sup>. However, Paris and de la Fuente<sup>11</sup> reported Pd values up to 5 due to the gel formation. They claimed the formation of lactones from the FT-IR results. According to Mennicken et al<sup>13</sup>, the cyclic polymerization suggested by Matsumoto is not significant and the crosslinking is due to the partial contribution of pendant allyl groups. They also reported the copolymerization of AMA with other monomers. Nagelsdiek et al<sup>14</sup> demonstrated that the gel formation is due to the degree of polymerization rather than crosslinking by allyl groups. The spectroscopic evidences do not show the presence of lactone groups ( IV and V). Liu et al<sup>15</sup> reported that AMA in copolymer gives the linear polymer with ally pendant groups. The reactivity ratios with other acrylates ( e.g. MMA) are compared. The detailed kinetic light induced polymerization of AMA is reported by Cohen et al<sup>16</sup>, the polymer obtained are partially soluble. The formation of polymer type III alone is not reported and the reactivity ratio is shown to be very small<sup>15</sup>. The

microgel-like PAMA were synthesized by emulsion polymerization, which gives polymers with pendant allyl groups<sup>17</sup>. The degradation of PAMA and its copolymers were studied by Zulfigar et al<sup>18-20</sup> using TGA, TVA, DTA and GC-MS methods. They have collected the degradation fragments and characterized them by FT-IR after separation of fragments by condensation. The main pyrolysis products were related to the nature of polymer chain.

### 1.7. AIM OF THIS STUDY

All the reported works about PAMA are concentrated on the possibility of crosslinking and/or cyclopolymerization with contribution of allyl groups. The suggested evidences are based mostly on the solubility properties. In this case, the solubility property of polymer was attributed to the linear nature of the polymer chain. Thus, the insolubility of polymer is suggested to be due to the crosslinking with allyl groups. The aim of this study is to clarify the mechanism of AMA polymerization and verify the possible formation of crosslinking and/or cyclopolymerization to yielding lactones.

In this work, polymerization of AMA was carried out by free radical initiators and via radiation under different conditions. The effect of crosslinking and molecular weight on solubility were tested. The polymer chain was characterized by FT-IR, NMR analysis and thermal investigations, which give more evidence related to crosslinking and lactones formation. The detailed thermal degradation of PAMA was also carried out by XPS, MS, TGA, and DLS analyses.

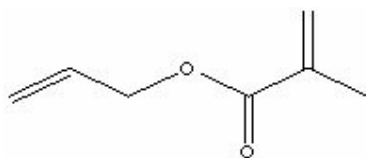
## CHAPTER 2

### 2. EXPERIMENTAL

#### 2.1. MATERIALS

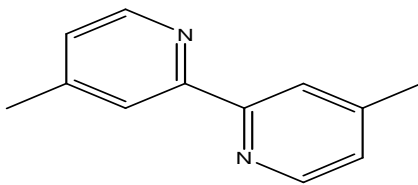
##### 2.1.1. Monomer

Allyl methacrylate, AMA (Aldrich) was purified via vacuum distillation at 31°C.



##### 2.1.2. Ligand

4,4'-dimethyl-2,2'-bipyridine (Fluka) was used as the ligand for atom transfer radical polymerization without further purification.

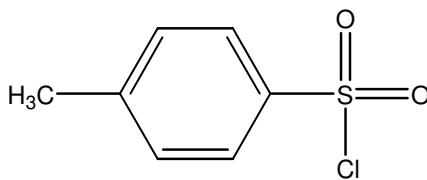


### 2.1.3. Catalyst

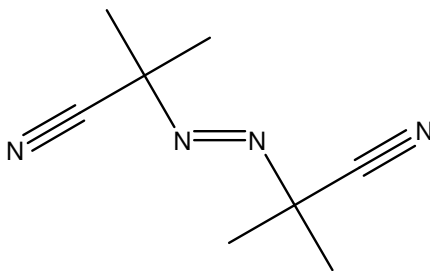
Copper(I) chloride (Riedel-de Haën) was used as the catalyst for atom transfer radical polymerization without further purification.

### 2.1.4. Initiator

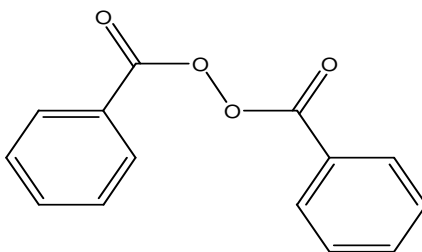
*p*-Toluenesulfonyl chloride (Aldrich) was used as the initiator for atom transfer radical polymerization without further purification.



*α,α'*-Azobisisobutyronitrile, AIBN (Merck) was used as the initiator for solution polymerization of AMA under vacuum without further purification.



Benzoyl peroxide, BPO (Merck) was used as the initiator for bulk polymerization of AMA in the presence of atmospheric oxygen without further purification.



### 2.1.5. Solvents

Methanol (Riedel-de Haën), toluene (Merck), carbon tetrachloride (Merck), dichloromethane (Lab-Scan) were all reagent grades and used without further purification.

## 2.2. INSTRUMENTATION

### 2.2.1. Polymerization Tubes

The polymerization tubes (Pyrex) were 1-3 cm in diameter and 10 cm in length. The open ends of the tubes were attached to another tube of smaller diameter, which allows to be connected to the vacuum line.

### 2.2.2. High Vacuum System

The polymerization tubes were evacuated at pressure of  $10^{-4}$  to  $10^{-5}$  mmHg for about 5-6 hours.

### 2.2.3. $^{60}\text{Co}$ $\gamma$ -Ray Source

The gamma radiation source was  $^{60}\text{Co}$  Gamma-cell 220 of Atomic Energy of Canada Ltd. Co. The source contains 12400 curie and has an intensity dose of 0.014 Mrad/h.

### 2.2.4. Infrared Spectrometer (FT-IR)

The FT-IR spectra of monomer and polymer samples were taken on a Perkin-Elmer Spectrum-1 FT-IR Spectrometer and on Bruker Vertex 70 ATR-FT-IR Spectrometer using KBr pellets.

### 2.2.5. Nuclear Magnetic Resonance (NMR)

$^1\text{H}$  and  $^{13}\text{C}$  NMR spectra of the monomer and polymers were taken on Bruker Ultrashield Digital 400 MHz NMR Spectrometer and Bruker Biospin High Resolution Digital 300 MHz NMR Spectrometer. Deuterated chloroform ( $\text{CDCl}_3$ ) was used as the solvent, and tetramethyl silane

(TMS) served as the internal standard. The solid state NMR used for insoluble polymer sample was Bruker Super Conducting FT-NMR Spectrometer, Avance TM 300 MHz WB with 4 mm MAS probe.

#### 2.2.6. Differential Scanning Calorimeter (DSC)

The DSC thermograms of the polymer samples were taken on a TA-DSC 910S differential scanning calorimeter with a heating rate of 5°C/min in the temperature range of 25 to 350°C under nitrogen gas atmosphere.

#### 2.2.7. Thermal Gravimetric Analysis (TGA-FT-IR)

TGA in situ FT-IR thermogram was taken on Perkin Elmer Pyris 1 TGA & spectrum 1 FT-IR Spectrometer under nitrogen gas atmosphere in a temperature range of 30-800°C with heating rate of 5°C/min.

#### 2.2.8. Mass Spectrometer (MS)

Mass spectrometer was Balzers QMG 311 quadrupole spectrometer with an electron impact of 70 eV. The scan rate of heating was 10°C/min starting at 25°C. The instrumental control and data acquisition were carried out by a computer.

#### 2.2.9. X-Ray Photoelectron Spectroscopy (XPS)

The X-ray Photoelectron Spectroscopy, XPS spectra were taken on Specs XPS using 200 W MgKa (1253.6 eV) under  $10^{-9}$  torr.

### 2.2.10. Dynamic Light Scattering (DLS)

Molecular weight of samples was taken on Malvern CGS-3 Dynamic Light Scattering, DLS.

### 2.2.11. Refractometer

The refractive index of PAMA in toluene solution at 25°C was measured by Bellingham + Stanley 60/70 ABPE refractometer.

### 2.2.12. X-Ray Powder Diffractometer (XRD)

X-Ray powder diffraction patterns (XRD) were taken using Rigaku Miniflex with Cu ( $K\alpha$  30 kV, 15 mA,  $\lambda=1.54178\text{\AA}$ ) radiation.

## 2.3. EXPERIMENTAL PROCEDURE

### 2.3.1. Bulk Polymerization of AMA via Chemical Initiation in the Presence of Atmospheric Oxygen

The reactants, 2 ml (15 mmol) AMA and 4 mg (0.0165 mmol) BPO, were placed in a Pyrex tube, which was sealed by flame without evacuation. It was then immersed in an oil bath at 70°C, polymerized for the desired period and then broken open. The content was dissolved in  $\text{CH}_2\text{Cl}_2$ , polymer was precipitated with excess methanol, filtered and dried under

vacuum at 40°C to constant weight. Conversions were calculated gravimetrically.

$$\% \text{ Conversion} = \frac{\text{Polymer Mass}}{\text{Monomer Mass}} \times 100$$

### 2.3.2. Solution Polymerization of AMA via Chemical Initiation under Vacuum

In a Pyrex tube, 2 ml (15 mmol) AMA, 5 mg (0.03 mmol) AIBN, and 4 ml CCl<sub>4</sub> were placed, and degassed via three freeze-pump-thaw cycles on the high vacuum system. The tube under vacuum was sealed by flame and placed in an oil bath at 50, 60 and 70°C, respectively for the desired period. They were then broken open; the polymer was precipitated by excess methanol. The rest of procedure was the same as 2.3.1. The insoluble fraction of polymer from 50°C was obtained by extracting polymer with toluene. For thermal pyrolysis, polymer sample in an evacuated test tube was heated at 280 and 350°C to constant weight. The FT-IR of residual polymer was recorded after removal of volatile degraded fragments.

### 2.3.3. Radiation Induced Bulk Polymerization of AMA in the presence of Atmospheric Oxygen

In a Pyrex tube, 2 ml (15 mmol) AMA were placed and sealed by flame without evacuation. The tube was placed in the  $\gamma$ -radiation source at

room temperature for the desired period. The rest of procedure was the same as (2.3.1).

#### 2.3.4. Radiation Induced Solution Polymerization of AMA under Vacuum

2 ml (15 mmol) AMA and 2 ml  $\text{CCl}_4$  were placed in a Pyrex tube, and degassed via three freeze-pump-thaw cycles on the high vacuum system in order to evacuate the tube. The tube under vacuum was sealed by flame and placed in the  $\gamma$ -radiation source at room temperature for the desired period. After irradiation, the tube was broken open, polymer precipitated by the addition of excess methanol. The rest of procedure was the same as (2.3.1).

#### 2.3.5. Radiation Induced Atom Transfer Radical Polymerization of AMA under Vacuum

The reactants, 2 ml (15 mmol) AMA, 15 mg (0.15 mmol)  $\text{CuCl}$ , 55 mg (0.30 mmol) 4,4'-dimethyl-2,2'-bipyridine, 28 mg (0.15 mmol) *p*-toluenesulfonyl chloride and 3 ml toluene were placed in a Pyrex tube. The rest of the experiment was the same as 2.3.4. The polymer was cleared from residual copper and percent conversions were calculated gravimetrically.

## **CHAPTER 3**

### **3. RESULTS AND DISCUSSION**

#### **3.1. POLYMERIZATION OF AMA**

##### **3.1.1. Polymerization of AMA via Chemical Initiation**

The bulk polymerization of AMA by BPO in the presence of atmospheric oxygen at 70°C was carried out and the percent conversions were calculated. The results are tabulated in Table 3.1 and plotted in Figure 3.1a. The kinetic curve is S-shape type and the polymerization showed an autoacceleration mechanism with an induction period of more than 0.3 h, which is due to the presence of oxygen in the sealed polymerization tube. After all the oxygen is consumed, the radical polymerized the monomer. The percent conversion reached to about 90% with a high rate, then the rate slows down up to limiting conversion of 100% in about 16 h. When the molecular weight of polymer reached to high values, the mobility of monomer molecules decreased and as a result, the rate of propagation also decreased (eq.1.2.5). The polymer obtained was colorless, transparent and brittle gel type. It was insoluble in common organic solvents. Insolubility of polymer may due to high

molecular weight in the early stage of polymerization and/or crosslinking by allyl groups.

**Table 3.1** Bulk polymerization of AMA by BPO in the presence of atmospheric oxygen at 70°C

Time (h)	% Conversion
0.25	0.00
0.50	2.60
0.75	1.80
1.00	4.30
1.17	8.90
1.33	10.30
1.40	50.00
1.50	80.70
1.75	83.40
2.00	84.90
2.25	87.3
2.50	87.1
2.75	88.6
3.00	88.9
15.75	99.2

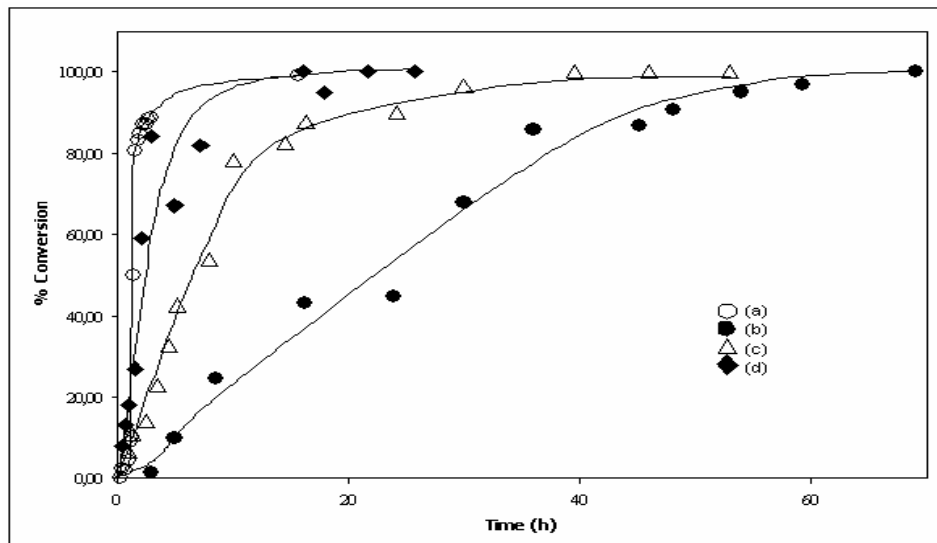


**Figure 3.1** Polymerization of AMA (a) in bulk by BPO in the presence of atmospheric oxygen at 70°C and in  $\text{CCl}_4$  by AIBN at (b) 50, (c) 60, and (d) 70°C

In order to obtain soluble, lower molecular weight polymers, polymerization was carried out in a solvent which has a higher chain transfer constant. The solution polymerization of AMA by AIBN in  $\text{CCl}_4$  under vacuum at 50, 60, and 70°C were carried out and the percent conversions were calculated. The results are tabulated in Tables 3.2, 3.3 and 3.4, and plotted in Figures 3.1b, c and d, respectively. Noticeable induction period is not observed in solution polymerization (Figures 3.1b, c, d) compared to bulk polymerization in the presence of atmospheric oxygen (Figure 3.1a). The autoacceleration is observed at 60 and 70°C but not at 50°C, where the percent conversion changes linearly up to about 90%. In solution polymerization, the percent conversion is reached to %100 at 50°C in 69 h, at 60°C in 39.50 h, and at 70°C in

21.67 h. This shows that the polymerization rate increased with increase of temperature. However, in bulk polymerization, the percent conversion is reached to %100 at 70°C in 15.8 h. Thus, the percent conversions obtained in solution polymerization are lower than those for bulk polymerization.

**Table 3.2** Solution polymerization of AMA by AIBN at 50°C

Time (h)	% Conversion	% Insoluble	$\ln[M]/[M_0]$
3.00	1.33	0.00	-0.0134
5.00	10.01	2.97	-0.1054
6.58	6.81	-	-0.0705
8.50	24.41	22.65	-0.2798
16.16	43.13	41.85	-0.5644
24.00	44.92	43.03	-
30.00	67.87	67.17	-
36.00	85.74	86.14	-
45.25	86.90	88.82	-
48.00	90.83	89.45	-
54.00	95.19	94.94	-
59.25	97.00	97.00	-
69.00	100.00	100.00	-

**Table 3.3** Solution polymerization of AMA by AIBN at 60°C

Time (h)	% Conversion	$\ln[M] / [M_0]$
0.90	6.64	-
1.25	10.89	-0.12
2.50	13.94	-0.15
3.50	22.87	-0.26
4.50	32.81	-0.4
5.25	42.76	-0.56
8.00	53.99	-
10.00	78.35	-
14.50	82.37	-
16.25	87.68	-
24.25	90.27	-
30.00	96.59	-
39.50	100.00	-
46.00	100.00	-
53.00	100.00	-

**Table 3.4** Solution polymerization of AMA by AIBN at 70°C

Time (h)	% Conversion	$\ln[M] / [M_0]$
0.50	7.96	-0.083
0.75	13.11	-0.1406
1.00	17.78	-0.1957
1.50	26.96	-0.3142
2.16	58.99	-
3.00	84.21	-
5.00	67.00	-
7.25	82.04	-
16.00	100.00	-
18.00	94.87	-
21.67	100.00	-
25.75	100.00	-

The percent of insoluble fraction in toluene against time at 50°C are tabulated in Table 3.2 and plotted in Figure 3.2. The polymers obtained are partially soluble at lower conversions. For example, at a total conversion of 10%, the insoluble fraction is about 3% (Figure 3.2). As the total conversion increases, the insoluble fraction also increases, reaching to 100%. Hence, the polymers obtained in solution polymerization are partially soluble compared to bulk polymerization at lower conversions.

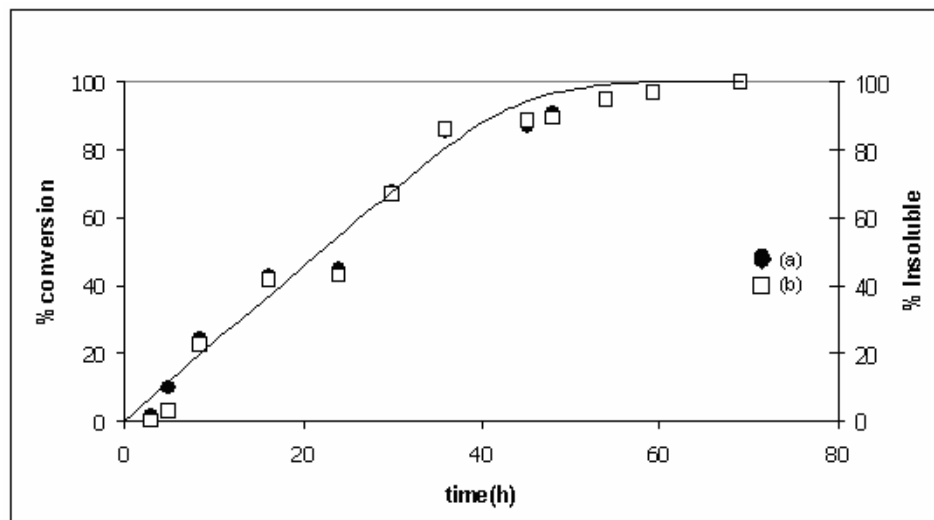


**Figure 3.2** The percent conversion (a) total and (b) insoluble fraction in toluene against time at 50°C

### 3.1.2. Radiation Induced Polymerization of AMA

The bulk polymerization of AMA by  $\gamma$ -radiation in the presence of atmospheric oxygen was carried out and percent conversions were calculated. The results are tabulated in Table 3.5 and plotted in Figure 3.3a. The kinetic curve is in the S-shape type and autoacceleration is observed. The tubes were sealed without removing  $O_2$ , which caused a considerable induction period of more than 5 h. The polymer obtained was mostly insoluble in common organic solvents.

**Table 3.5** Radiation induced bulk polymerization of AMA in the presence of atmospheric oxygen

Time (h)	% Conversion
1.92	0.00
4.83	0.00
16.50	0.30
50.67	6.20
65.00	24.20
73.00	63.40
89.50	65.50
102.58	79.50
137.91	78.60
165.00	82.50
192.67	97.30

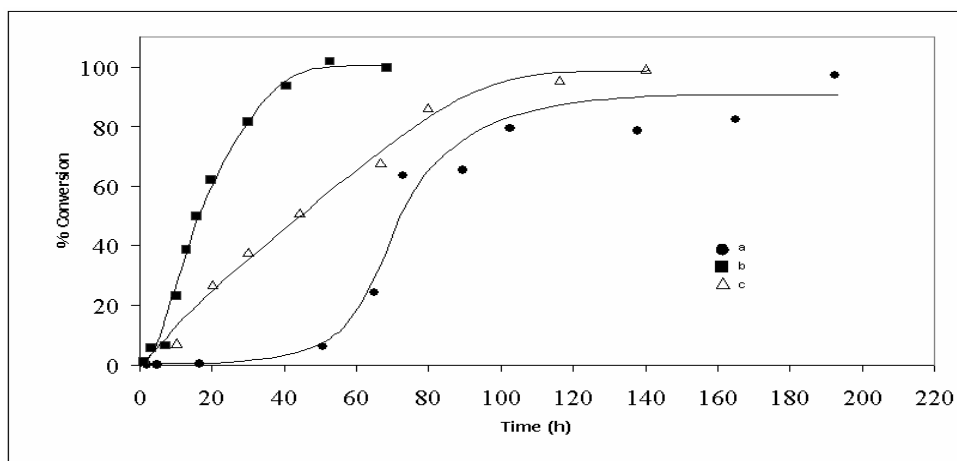


**Figure 3.3** Radiation induced polymerization of AMA (a) in bulk in the presence of atmospheric oxygen, (b) in CCl<sub>4</sub> solution under vacuum, and (c) ATRP under vacuum

The solution polymerization of AMA in  $\text{CCl}_4$  by  $\gamma$ -radiation under vacuum was carried out and percent conversions were calculated. The results are tabulated in Table 3.6 and plotted in Figure 3.3b. The rate of polymerization was high and the curve obtained was almost linear up to limiting conversion. The polymer obtained was mostly insoluble in common organic solvents.

**Table 3.6** Radiation induced solution polymerization of AMA under vacuum

Time (h)	% Conversion
1	1.02
3	5.66
7	6.5
10	23.19
13	38.63
15.75	49.96
19.58	62.04
30	81.59
40.50	93.68
52.58	100.00
68.41	99.81

In the conventional ATRP method, the reactants are mixed and initiated thermally. However, polymerization reaction is highly exothermic and the boiling point of AMA is  $140^\circ\text{C}$ . The high temperature will also start the polymerization and cause the crosslinking. In order to avoid the high temperature effect, ATRP method was initiated with radiation. The ATRP

of AMA by  $\gamma$ -radiation under vacuum was carried out and percent conversions were calculated. The results are tabulated in Table 3.7 and plotted in Figure 3.3c. The curve obtained was almost linear with respect to time and different from radiation induced bulk polymerization which usually gives autoacceleration kinetics. Therefore, the temperature did not interfere with the polymerization kinetics and the crosslinking caused by thermal curing was avoided. This showed that the molecular weight of polymer obtained by the radiation induced polymerization of AMA can be controlled. The polymers obtained by all of the polymerization methods carried out were mostly insoluble showing that molecular weight increased in early stage of polymerization.

**Table 3.7** Radiation induced atom transfer radical polymerization of AMA under vacuum

Time (h)	% Conversion
10	7.33
20.25	27.1
30	37.85
44.25	51.06
66.67	67.86
80	86.21
116.25	95.53
140	99.55

In solution and ATRP methods, induction period and autoacceleration are not observed compared to bulk polymerization. The percent conversion reached to %100 in 192.62 h in bulk polymerization, 68.41 h in solution polymerization and 140 h in ATRP. The curves obtained were almost linear up to 62.04% in solution polymerization and 86.21% in ATRP. The rate of bulk polymerization after induction period is the same as that of the solution polymerization. The polymer obtained by ATRP had more soluble fractions compared to those obtained for other methods.

### 3.1.3. Arrhenius Activation Energy for Chemically Initiated Polymerization of AMA

Arrhenius plot was used to calculate the activation energy of solution polymerization of AMA using initial rate constant of 50, 60, and 70°C. The rate constants were calculated from kinetic equation (1.2.6).  $\ln [M] / [M_0]$  values (Tables 3.2-4) versus time for 50, 60, and 70 °C are plotted in Figures 3.4a, b, and c, respectively and slopes (k values) were calculated for each of polymerization temperature. The results are tabulated in Table 3.8. Then,  $\ln k$  versus  $1/T(K)$  is plotted in Figure 3.5. The Arrhenius activation energy calculated from the slope is 82.3kJ/mol. This value of activation energy showed that the polymerization takes place by radical mechanism.

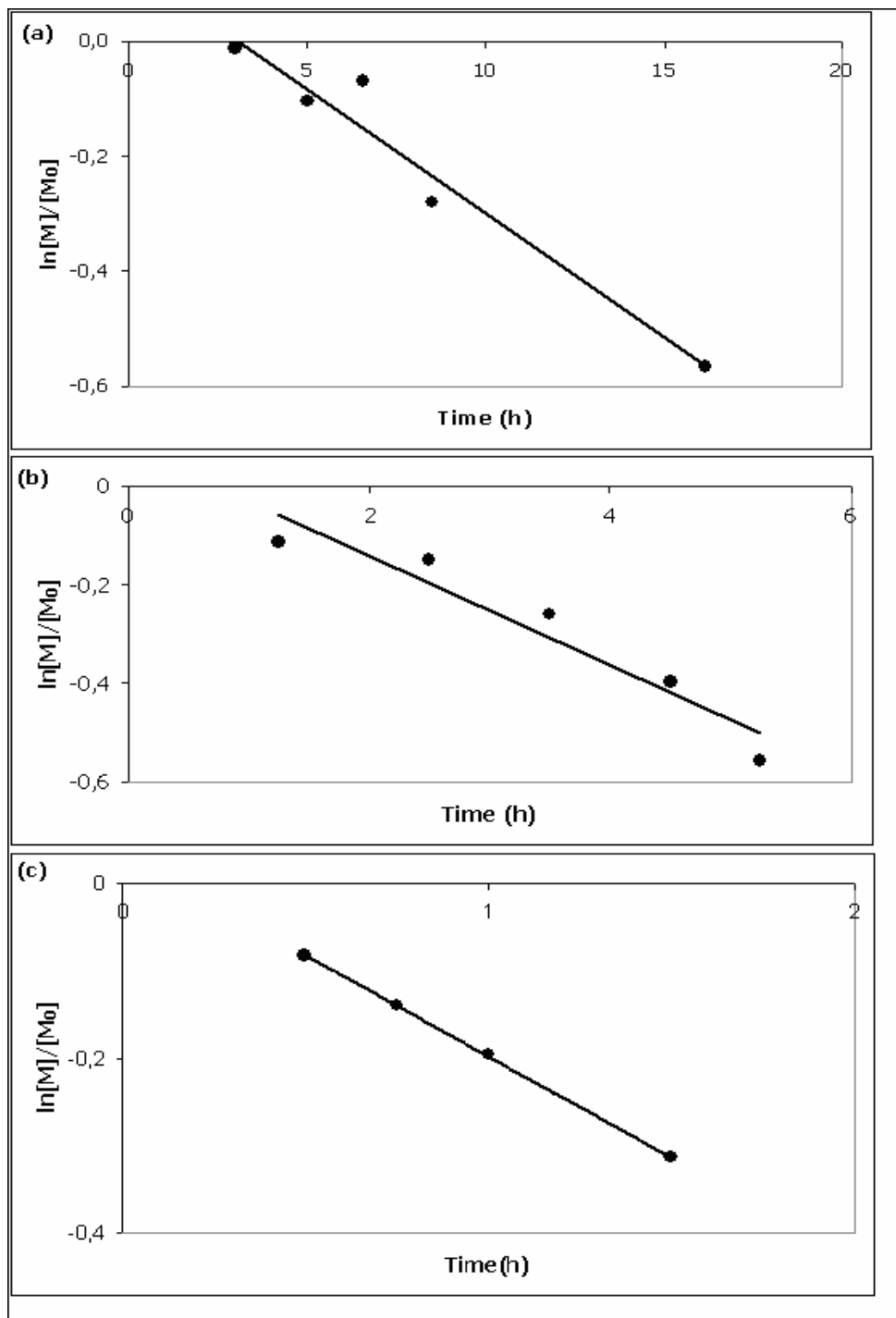


**Figure 3.4** The plots of  $\ln[M]/[M_0]$  vs. time for solution polymerization at (a) 50, (b) 60, and (c) 70°C

**Table 3.8** Reaction rate constants for solution polymerization of AMA

T(K)	1/T(K <sup>-1</sup> )	k=Slope (h <sup>-1</sup> )	ln k
323	0.00309	0.043	-3.1465
333	0.00300	0.1104	-2.2036
343	0.00292	0.231	-1.4653

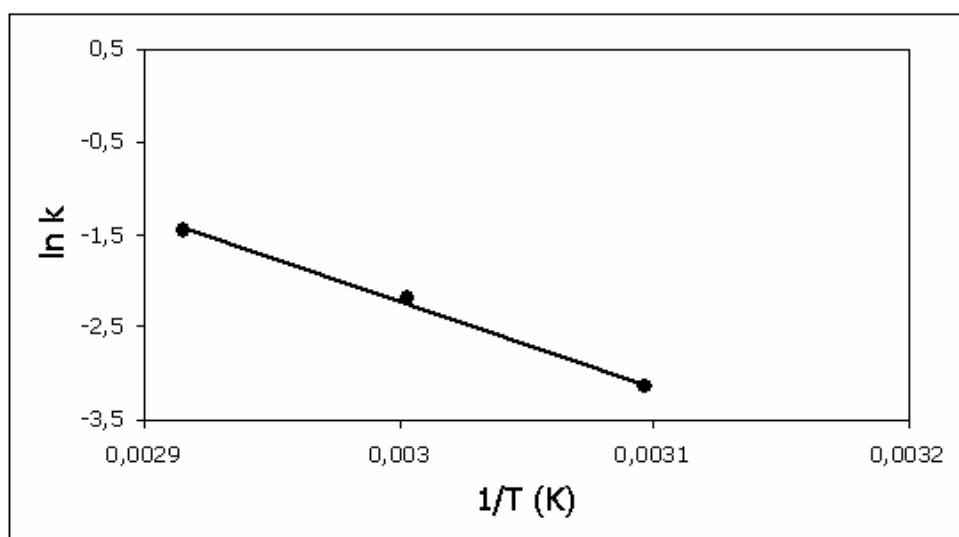


**Figure 3.5** ln k vs 1/T

## 3.2. CHARACTERIZATION OF PAMA

### 3.2.1. FT-IR Investigation

The FT-IR spectrum for AMA and PAMA are shown in Figures 3.6a and b, respectively and the peak assignments are tabulated in Table 3.9. The FT-IR spectra of polymers obtained under different conditions were identical and they did not change with percent conversion.

**Table 3.9** The peak assignments for the FT-IR spectrum of AMA and PAMA

Functional Group	Shift (cm <sup>-1</sup> )	
	AMA	PAMA
=CH-	3087.97, 3019.24	3087.40
C-H in -CH <sub>3</sub>	2985.26, 2956.97	2988.24
C-H in -CH <sub>2</sub> -	2930.76	2940.42
C-H in -OCH <sub>2</sub> -	2886.92	2848.00
-C=O	1722.59	1728.83
-C=C-	1638.54 (vinyl and allyl)	1647.52 (allyl)
-CH <sub>2</sub> -	1453.66, 1403.67	1471.64
-CH <sub>3</sub>	1379.93, 1361.75, 1318.80, 1297.60	1389.86, 1262.35
-C-O-C-	1164.37, 1013.05	1145.48
-CH=C- (allyl)	986.00, 937.92	982.18, 930.76
-CH=C- (vinyl)	814.41	-

In the spectrum of PAMA (Figure 3.6b), the allyl peaks observed at 3087.40, 1647.52, 982.18 and 930.76  $\text{cm}^{-1}$  are retained with a decrease in intensity due to vinyl group disappearance. The specific vinyl peak at 814.4  $\text{cm}^{-1}$  disappeared completely. This showed that polymerization is proceeding on vinyl, where allyl groups are not mainly involved in polymerization reaction. The insoluble nature of polymer is due to the high molecular weight and/or crosslinking for a certain extent due to allyl groups. In order to understand whether crosslinking occurred during polymerization as suggested by Zhang and Ruckenstein<sup>3</sup>, the percentage of allyl groups used in polymerization was calculated by taking the ratio of absorption intensity of olefinic peak to the carbonyl peak. The corresponding ratio of the absorbance after polymerization decreased to about 25% which is different from 50%<sup>3</sup>. However, the FT-IR peak intensity depends on the dipole moment of the bond, which is different for allyl and vinyl groups. Therefore, the direct contribution of vinyl and allyl group absorbance intensities to the total absorbance is not 1:1 as claimed in literature<sup>3</sup>. Thus, certain extents of allyl groups could be used for crosslinking during polymerization, which can be predicted from NMR results.

The lactones and anhydride peaks should be observed at 1750-1850  $\text{cm}^{-1}$  in FT-IR spectrum. However, these peaks are not observed in the spectrum of PAMA (Figure 3.6b). Therefore, either these groups are not present in the polymer chain at all or they are in very small quantities. They can be predicted from the NMR results which have higher resolution power.

FT-IR spectra of soluble PAMA fraction from polymerizations with conversion of 10, 45 and 79% are shown in Figures 3.7b, c and d, respectively. In the spectrum of 10.01% conversion PAMA (Figure 3.7b),

the peak for the –CN (initiator) was observed at 2350-2360  $\text{cm}^{-1}$ . The solvent C-Cl peak was observed at 750  $\text{cm}^{-1}$ . Since the molecular weight of PAMA is very high, the end group cannot be detected in FT-IR spectra. However, the soluble fractions which can be low molecular weight polymers and/or oligomers, gives high enough end groups that can be observed. Therefore, the presence of –CN group and solvent at the end group can be observed in FT-IR spectra. This was also confirmed by MS and ESCA results. The same modifications were also observed for the polymers of 45% and 79% conversions. The main difference observed was in the relative intensity of peaks as the conversion increases.

The PAMA sample was thermally treated at different temperatures to observe the possible side group cyclization yielding lactones and/or anhydride. FT-IR spectrum of residual PAMA after pyrolysis at 280 and 350°C are given in Figures 3.8a and b, respectively. The allyl peaks after thermal treatment at 280°C retained their position with a decrease in intensity. After 350°C, the allyl groups almost disappeared and the anhydride and/or lactones carbonyl peak appeared at 1771.5  $\text{cm}^{-1}$ . Thus, at about 350°C the linkage degradation of side groups in the polymer chain is maximized with the possible formation of anhydride and/or end group cyclization to lactones. The details of fragmentation are obtained from MS and TGA thermograms. The intensity of C-Cl peak at 752  $\text{cm}^{-1}$  (Figure 3.8a) decreased as given in Figure 3.8b.

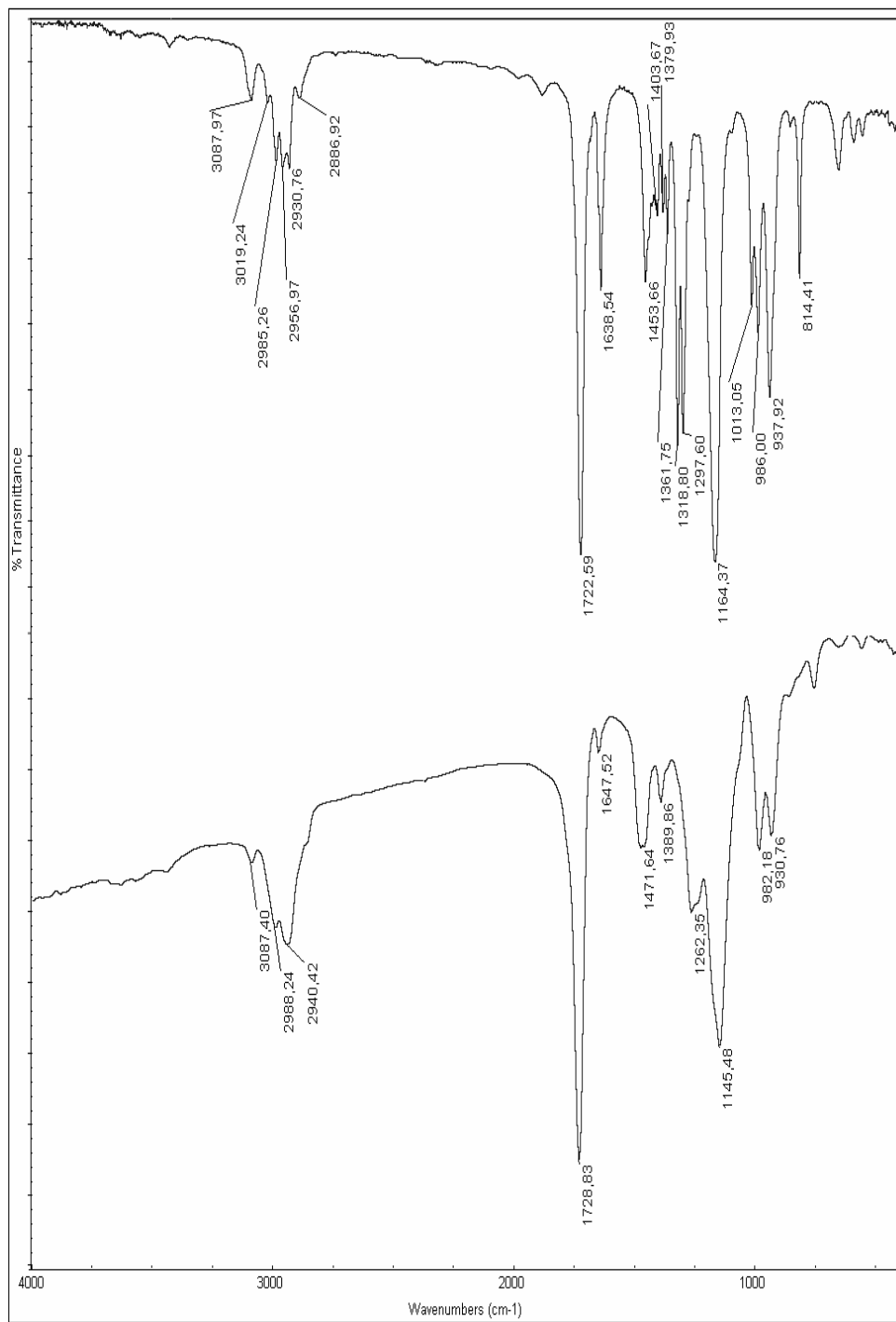


**Figure 3.6** FT-IR spectra of (a) AMA, (b) PAMA from bulk polymerization by BPO in the presence of atmospheric oxygen (80.7%)

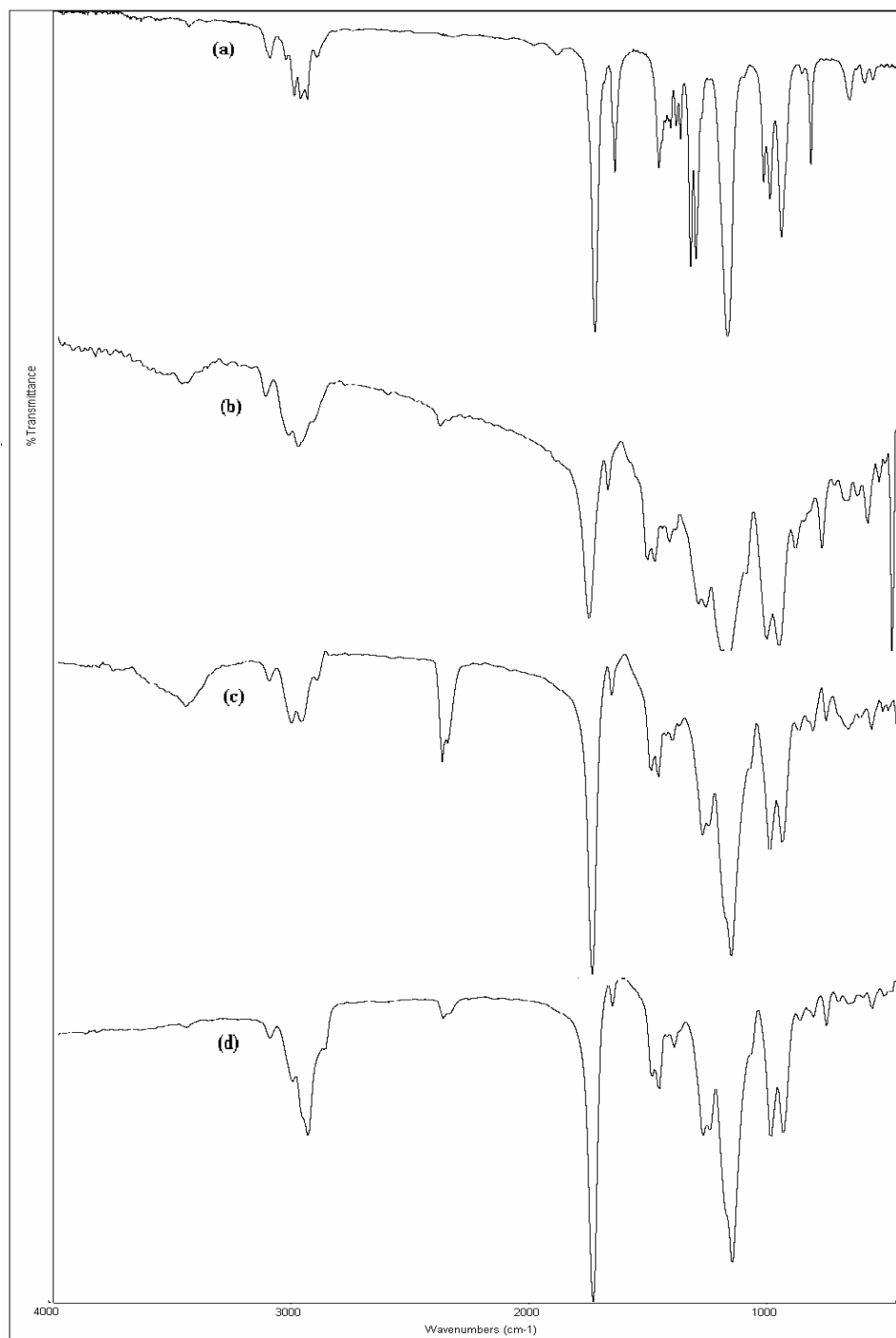


**Figure 3.7** FT-IR spectra of (a) AMA and soluble PAMA fraction from solution polymerization by AIBN under vacuum with a conversion of (b) 10%, (c) 45%, (d) 79%

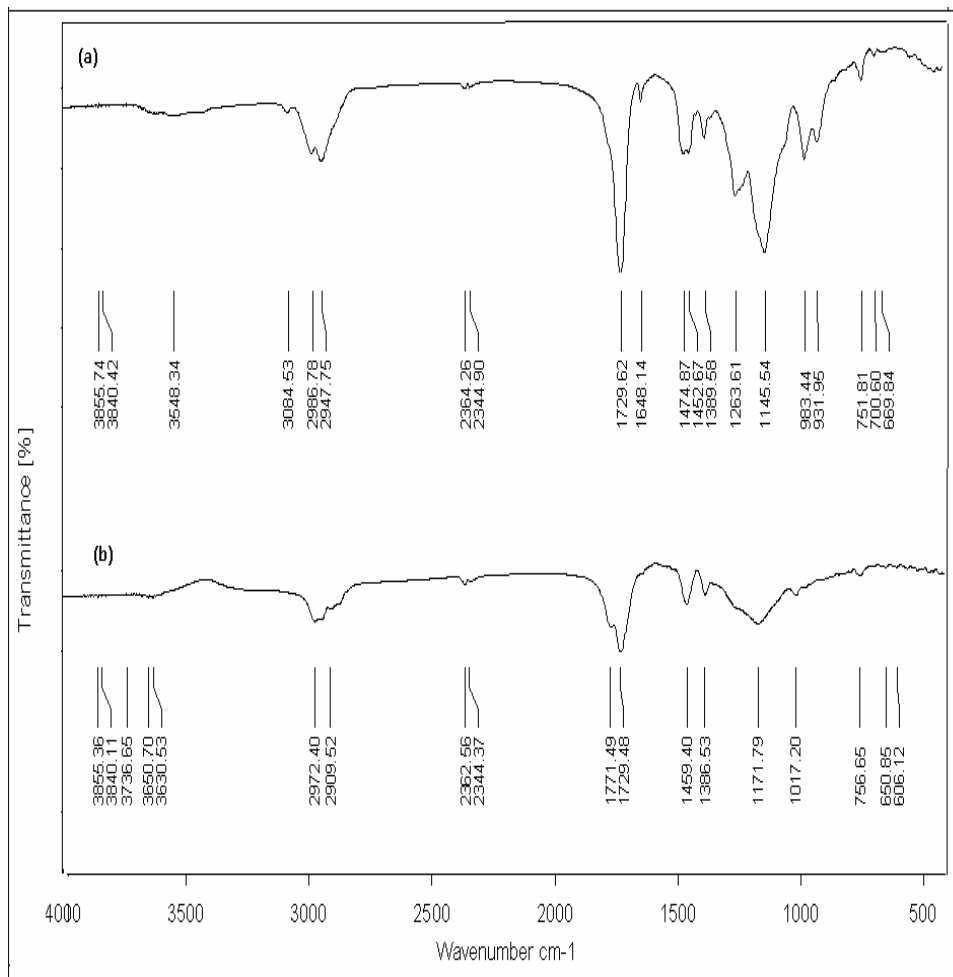


**Figure 3.8** FT-IR spectra of residual PAMA pretreated at (a) 280 and (b) 350°C

### 3.2.2. NMR Investigation

$^1\text{H}$ -NMR spectrum of AMA and PAMA are given in Figures 3.9a and b, respectively, and the peak assignments are tabulated in Table 3.10.

**Table 3.10**  $^1\text{H}$ -NMR spectrum of AMA and PAMA

Proton Type	Shift (ppm)	
	AMA	PAMA
$-\text{CH}_3$	1.96	0.80-1.00
$-\text{OCH}_2-$	4.64	4.40
$-\text{CH}=\text{CHH}$	5.21-5.24	5.15-5.20
$-\text{CH}=\text{CHH}$	5.31-5.35	5.25-5.30
$\text{CH}_2=\text{C}(\text{CH}_3)-$	5.56-6.12	-
$-\text{CH}_2-\text{C}(\text{CH}_3)-$	-	1.12-1.70
$-\text{CH}=\text{CH}_2$	5.90-6.00	5.85-6.00
$-\text{O}-\text{CH}_2-\text{CH}_2-\text{CH}_2-$	-	3.70
$-\text{O}-\text{CH}_2-\text{CH}_2-\text{CH}_2-$	-	1.3-1.4
$\text{CDCl}_3$	-	7.2

The peaks of vinyl hydrogens in AMA (5.56, and 6.12 ppm) were replaced by single C-C bond hydrogen peaks (1.12 and 1.70 ppm). The  $-\text{CH}_3$  peak shifted to 0.80-1.00 ppm after opening of vinyl group. However, the peak positions of allyl groups (5.21-5.24; 5.31-5.35 and 5.90 ppm) in AMA were not changed after polymerization (5.15-5.20; 5.25-5.30 and 5.85 ppm, PAMA). These results showed that allyl groups were remained as pendant groups in polymer chains while vinyl double

bond was opened. The hydrogen peak intensity calculations (Figure 3.9) showed that about 98-99% of the allyl groups were retained in PAMA. About 1 to 2% allyl groups were altered into crosslinking and/or lactones formation. This is proved by the observed methylene (-O-CH<sub>2</sub>-CH<sub>2</sub>-) peak of allyl group at 3.7 ppm in crosslinked PAMA. The pendant allyl (-O-CH<sub>2</sub>-CH<sub>2</sub>-CH<sub>2</sub>-) groups were in the range of 1.3-1.4 ppm as multiplet. Therefore, a very small amount of the allyl groups were involved in crosslinking. Since conversion for this polymer sample is about 58.83%, the crosslinking has a very limited contribution from allyl groups for polymerization. If five- or/and six-membered lactones were present, the proton peaks would be at 2.07, 4.14, 4.39 ppm (quartet); anhydride peaks at 1.52, 1.54 and 1.79 ppm (multiplet) which do not exist in the spectrum. Therefore, there are no lactones or anhydride groups in the polymer chain. The FT-IR and NMR results showed that even at 100% conversion the allyl groups have contributed to the crosslinking and/or cyclization at the extent of about 1-2%. As a result, the insoluble nature of polymer is due to the high molecular weight even in the early stages of polymerization rather than crosslinking. This is also supported by DLS.

The <sup>1</sup>H-NMR spectra of polymers for different polymerization conditions were identical. The only difference in soluble PAMA from solution polymerization by AIBN is the -CH<sub>3</sub> peak from initiator at 1.27 ppm, which is given in Figure 3.10.

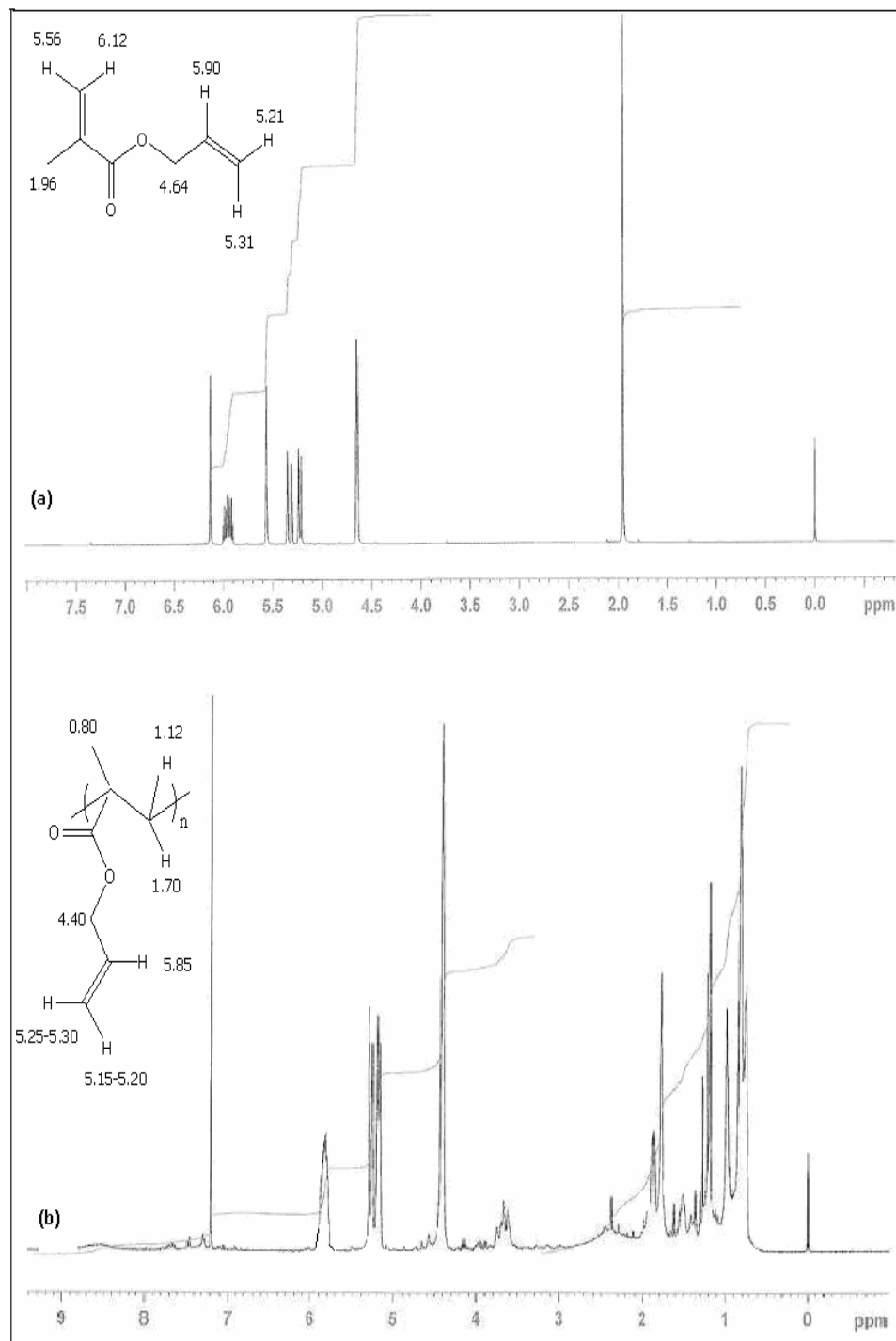


**Figure 3.9**  $^1\text{H-NMR}$  spectra of (a) AMA, (b) PAMA from ATRP under vacuum (58.83%)

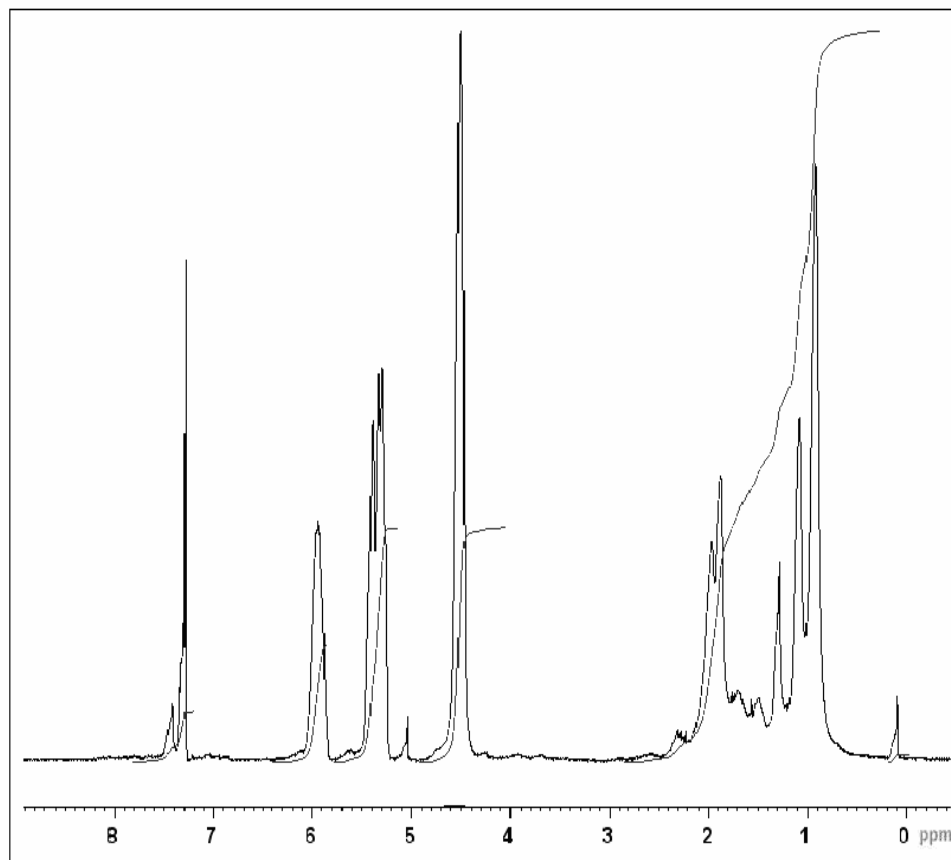


**Figure 3.10**  $^1\text{H}$ -NMR spectrum of soluble PAMA fraction from solution polymerization by AIBN under vacuum at 50°C (44.92%)

$^{13}\text{C}$ -NMR spectrum of AMA and solid state  $^{13}\text{C}$ -NMR spectrum of PAMA are given in Figures 3.11a and b, respectively and the peak assignments are tabulated in Table 3.11.

**Table 3.11**  $^{13}\text{C}$ -NMR spectrum of AMA

Functional Groups	Shift (ppm)	
	<b>AMA</b>	<b>PAMA</b>
-CH <sub>3</sub>	18.32	14.22
-OCH <sub>2</sub> -	65.27	63.42
-CH=CH <sub>2</sub>	117.88	116.66
CH <sub>2</sub> =C(CH <sub>3</sub> )-	125.49	-
-CH <sub>2</sub> -C(CH <sub>3</sub> )-	-	42.51
-CH=CH <sub>2</sub>	132.48	130.13
CH <sub>2</sub> =C(CH <sub>3</sub> )-	136.45	-
-CH <sub>2</sub> -C(CH <sub>3</sub> )	-	52.96
-C=O	166.95	174.33
-O-CH <sub>2</sub> -CH <sub>2</sub> -CH <sub>2</sub> -	-	80
-O-CH <sub>2</sub> -CH <sub>2</sub> -CH <sub>2</sub>	-	30
CDCl <sub>3</sub>	77(triplet)	77 (quartet)

The vinyl peaks in the spectrum of AMA (125.49 and 136.45 ppm) were shifted to the positions of 42.51 and 52.96 ppm, respectively in the spectrum of PAMA. Therefore, the vinyl bonds were involved during the polymerization. However, the peaks corresponding to the allyl group at 132.48 and 117.88 ppm in the spectrum of AMA were retained their position with small shifts (130.13 and 116.66 ppm). This is in agreement with FT-IR and  $^1\text{H}$ -NMR results that allyl groups are not contributing to

the polymerization process. Very small amounts of allyl groups were involved yielding crosslinking to a certain extent. The opened carbons of allyl groups give very weak peaks at 80 ppm (-O-CH<sub>2</sub>-**C**H<sub>2</sub>-CH<sub>2</sub>-) and 30 ppm (-O-CH<sub>2</sub>-CH<sub>2</sub>-**C**H<sub>2</sub>). The five- and/or six-membered lactones give peaks at about 40.2, 42.4, 58, 70.1 ppm and anhydrides at 40.0, 36.1, 32.1 ppm. However, these peaks were not observed in the spectrum of PAMA. Therefore, during the polymerization, considerable amounts of lactones or anhydrides were not formed.

The <sup>13</sup>C-NMR spectra of polymers obtained from different polymerization conditions were identical. The only difference in soluble PAMA from solution polymerization by AIBN is C atom from initiator, (CH<sub>3</sub>)<sub>2</sub>**C**(CN)- at 16.8 ppm; (CH<sub>3</sub>)<sub>2</sub>**C**(**C**N)- at 119.0 ppm, which is given in Figure 3.12a. The quartet nature of chloroform peak (triplet) at 77 ppm is due to the presence of -**C**Cl<sub>3</sub> arising from the solvent. The results showed that polymerization proceeded on the vinyl group with the initiator at the end of the chain and/or oligomers. The presence of -CN and solvent -Cl is in agreement with MS data proving the presence of oligomers.

In order to understand the formation of lactones and/or anhydrides, the solid state <sup>13</sup>C-NMR spectrum of residual PAMA after pyrolysis at 350°C is also given in Figure 3.12b. In this spectrum, the peaks (Figure 3.11b) for the allyl groups became broader. The peaks for anhydride at 32.6, 36.1 and 40.1 ppm were appeared in the spectrum. The broad peak of -C=O at 240 ppm indicates the formation of anhydrides. Since the peaks are very broad a conclusive remarks cannot be made for the presence of lactones.

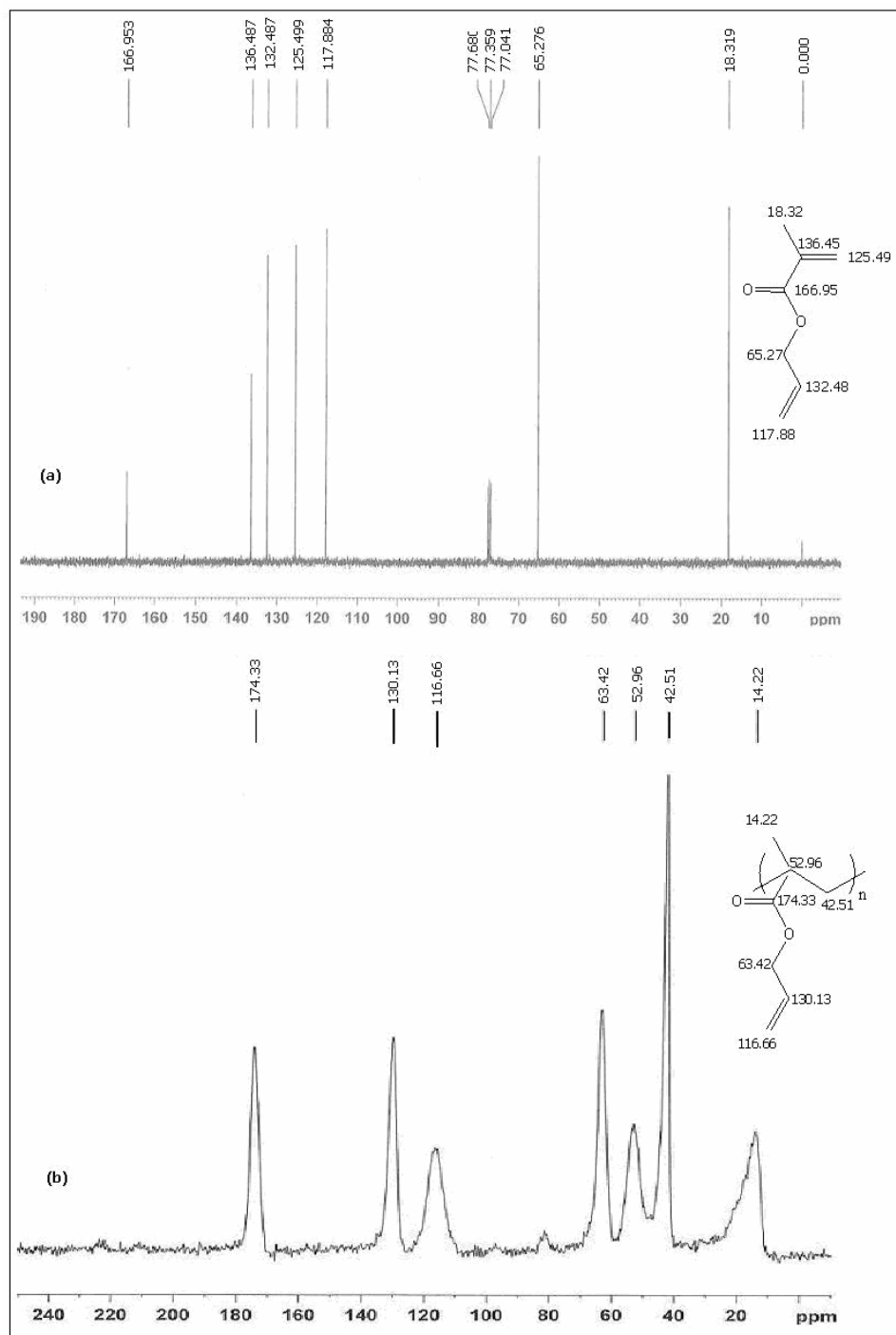


**Figure 3.11**  $^{13}\text{C}$ -NMR of (a) AMA and (b) PAMA from radiation induced solution polymerization under vacuum (99.81%)

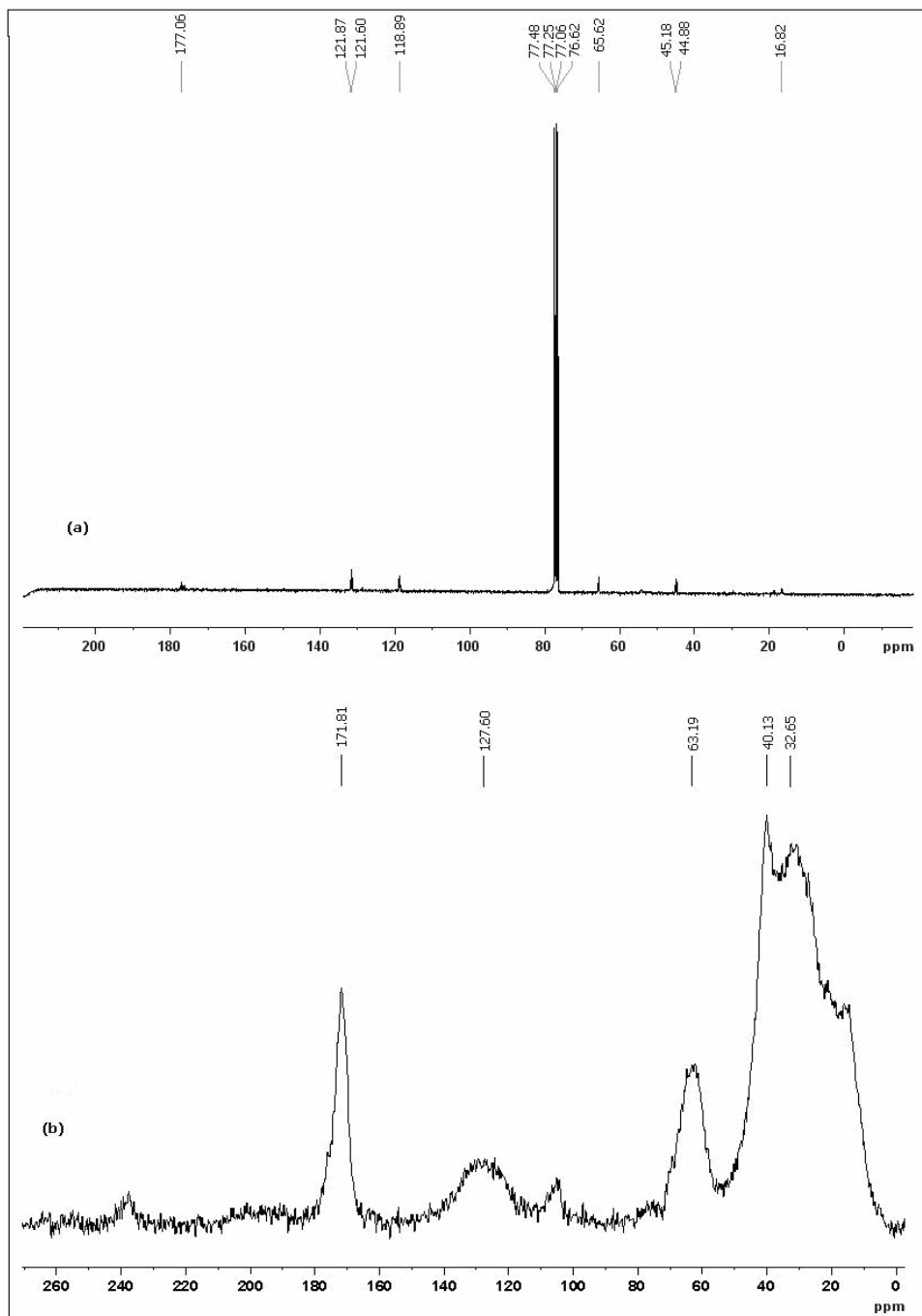


**Figure 3.12**  $^{13}\text{C}$ -NMR of (a) soluble PAMA fraction from solution polymerization by AIBN under vacuum at 50°C (44.92%) and (b) residual PAMA after pyrolysis at 350°C

### 3.2.3. DSC Investigation

The DSC thermograms of first and second runs for the polymer with 93.68% conversion are given in Figures 3.13a and b, respectively. The thermograms for other polymer conversions were very similar to the given thermograms. In the first run, broad exothermic peak centered at about 175°C showed the curing (further polymerization and crosslinking). The crosslinking is most probably due to the opening of some allyl groups. The Tg of polymer overlapped with the one peak for curing, therefore could not be observed. In the second run, the thermogram did not show any peak. This is because of the completion of curing in the first run. Therefore, the insolubility of PAMA is due to the high molecular weight observed even at very low conversions.

The DSC thermogram of PAMA did not give a Tg value. However, the thermograms of first and second runs for soluble PAMA, (Figures 3.14a and b) have a Tg value. A broad exothermic peak (100-160°C) centered at 154.86°C is due to the curing (further polymerization or crosslinking). The other peaks corresponding to Tg values are not very distinct in this thermogram. However, the derivative of the peak showed two Tg values at about 94 and 211°C. In order to understand the nature of endothermic peak, a second run was taken. The endothermic peak disappeared and a Tg is observed at 211°C. Therefore, the polymer without thermal treatment has a Tg value of about 94°C before curing and after curing, the Tg increased to 211°C.

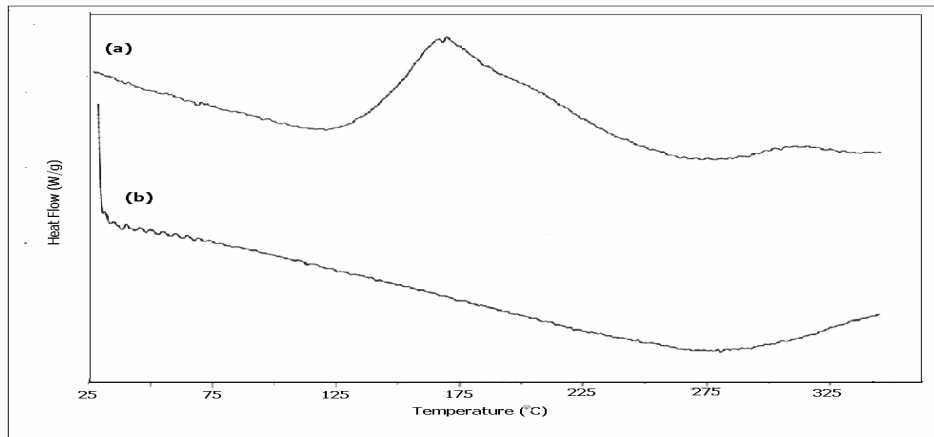


**Figure 3.13** DSC thermograms of PAMA (a) first run and (b) second run from radiation induced polymerization under vacuum (93.68%).

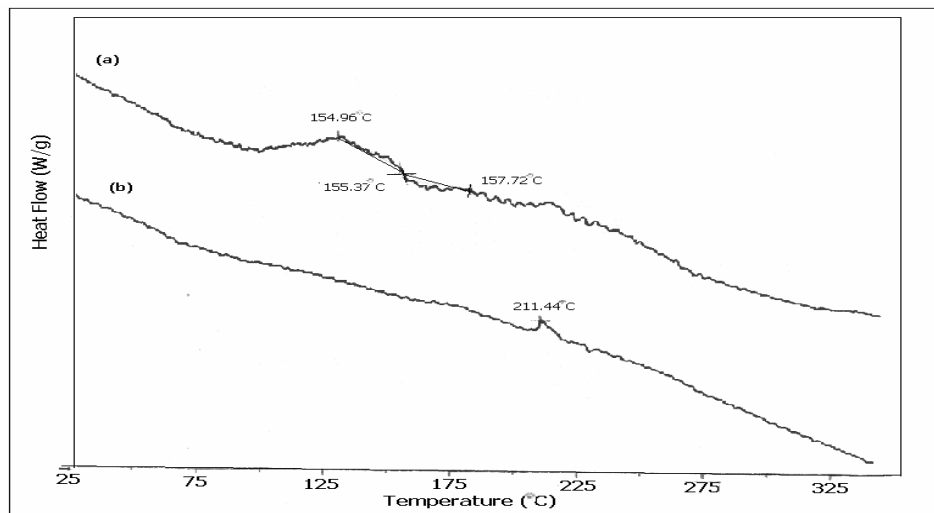


**Figure 3.14** DSC thermograms of soluble fraction of PAMA (a) first run and (b) second run from solution polymerization under vacuum at 50°C (71.36%)

### 3.2.4. TGA Investigation

The TGA thermogram of insoluble fraction of PAMA is given in Figure 3.15 in the temperature range of 30-800°C. The FT-IR spectrum of degraded fragments at 271, 343, 402 and 417°C are given in Figures 3.16a, b, c and d, respectively. The TGA thermogram showed two-stage degradation. Degradation started above 100°C, continued up to 220°C with a slower rate, then faster after 220°C, maximized at 266°C. The first stage (220-340°C) is linkage type degradation (fragmentation I and II) and the products are CO, CO<sub>2</sub>, CN, -CH<sub>2</sub>-CH=CH<sub>2</sub>, -O-CH<sub>2</sub>-CH=CH<sub>2</sub>, -C(=O)-O-CH<sub>2</sub>-CH=CH<sub>2</sub> and anhydride (Figures 3.16a and b). The results are in agreement with the FT-IR data given in Figure 3.8. In the second-stage (350-500°C), thermal degradation is mostly depolymerization type and further degradation of anhydride is observed (fragmentation III). The main fragmentation products are that of monomer which is formed by end group cyclization (fragmentation IV, V and VI). The monomer molecule is not observed in the FT-IR spectrum of fragments (Figures 3.16c and d). Therefore, the monomer is thermally unstable and easily fragmented further which was in agreement with MS data.



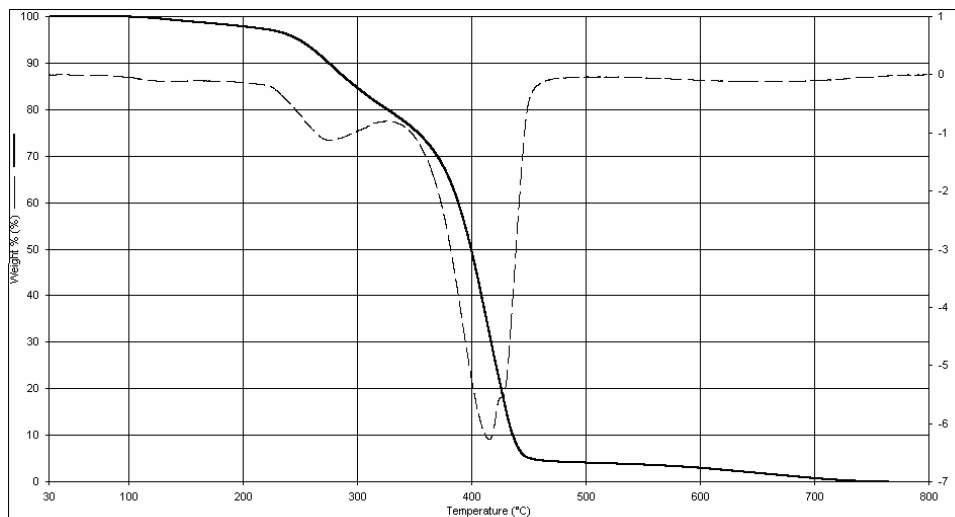


**Figure 3.15** TGA thermogram of insoluble PAMA fraction from solution polymerization by AIBN at 50°C (67.87%)

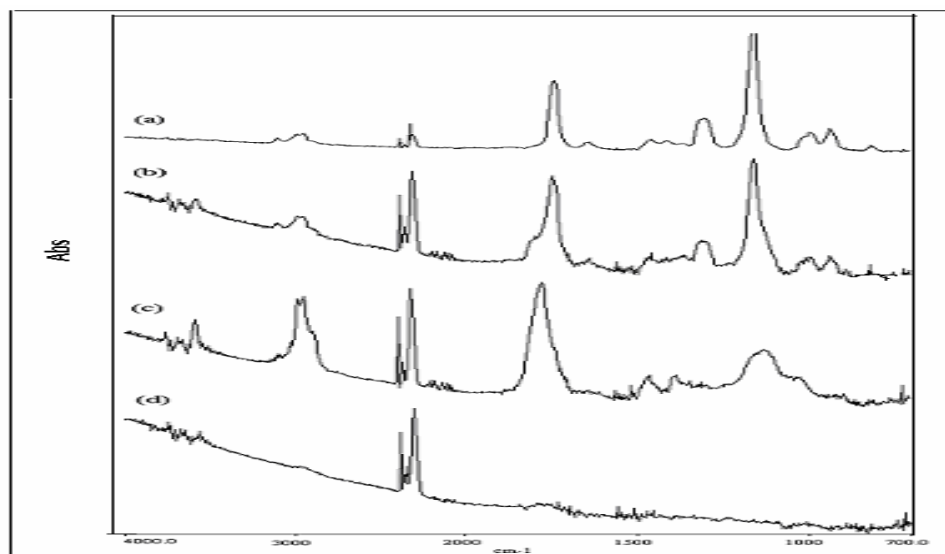


**Figure 3.16** FT-IR spectra of TGA degradation fragments of PAMA at (a) 271, (b) 343, (c) 402, and (d) 417°C

The TGA thermogram for soluble fraction of PAMA is given in Figure 3.17 in the temperature range of 30-900°C. The FT-IR spectrum of degradation fragments at 225, 387 and 579°C are given in Figures 3.18a, b and c, respectively. The TGA thermogram showed three degradation stages. The weight loss started at about 100°C, became sharper after 200°C, maximized at 250°C. The first stage (220-340°C) is linkage type degradation. At 225.69°C, FT-IR spectrum showed the fragments corresponding to allyl groups at 3084.5, 1648.1 and 931.9  $\text{cm}^{-1}$ ; CO, CO<sub>2</sub> and CN at 2200-2300  $\text{cm}^{-1}$ ; carbonyl corresponding to ester anhydride, and lactones at 1720-1850  $\text{cm}^{-1}$ ; ether and ester at 1100-1300  $\text{cm}^{-1}$ . In the second stage (300-410°C) thermal degradation is mostly depolymerization type and monomer does not appear as a fragment, but is fragmented into components as also proven by MS data. Thus, in TGA analysis, the polymer is depolymerized to give monomer which is immediately degraded to its fragments. At 387°C, FT-IR spectrum gives similar fragmentation with increase of peak intensity for CO, CO<sub>2</sub> and CN and peak broadening of carbonyl group. This can be due to the anhydride and lactones formation which fragmented to give more CO and CO<sub>2</sub> (fragmentation III). The third stage (410-590°C) is random scission degradation. At 579°C the emission of CO and CO<sub>2</sub> is almost completed and the most important fragments are ether or ester type. At this stage, the emissions of OH and NH groups are also noticeable and the complete fragmentation reaches to about 97%. Therefore, the degradation is almost completed at about 600°C.

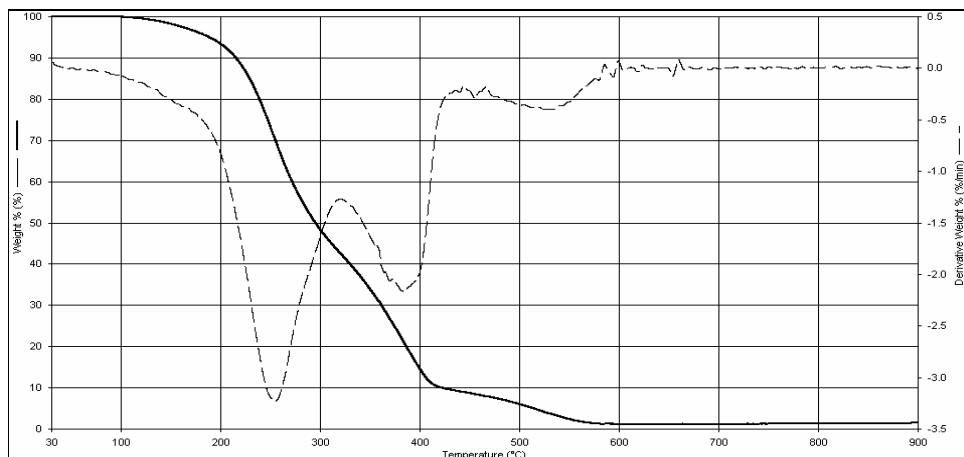


**Figure 3.17** TGA thermogram of soluble PAMA from solution polymerization by AIBN at 50°C (67.66%)

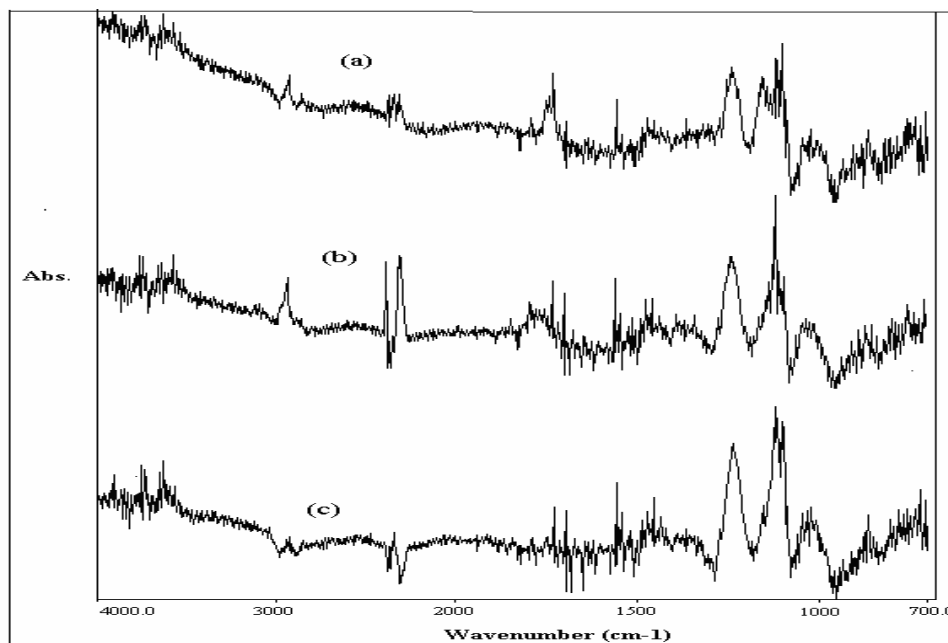


**Figure 3.18** FT-IR spectra of TGA degradation fragments of PAMA at (a) 225, (b) 387, and (c) 579°C

### 3.2.5. MS Investigation

The mass spectra of insoluble and soluble PAMA are given in Figures 3.19a and b, respectively. The fragmentation in each of the thermogram shows two regions at about 225-350°C and 395-515°C. The first peak is broader and mostly due to the linkage breakage of pendant allyl groups. The intensity of the second peak is higher, which shows the main polymer chain scissoring and/or depolymerization followed by fragmentation at this temperature range. The small difference between the two thermograms is in the peak shape and positions. Especially, the first peak area in the soluble PAMA (Figure 3.19b) is larger because the pendant groups can be easily fragmented. The second peak area (Figure 3.19a) is larger and extends to higher temperatures for insoluble PAMA. The broad peak at 25-125°C in both spectra corresponds to the impurities (excess background).

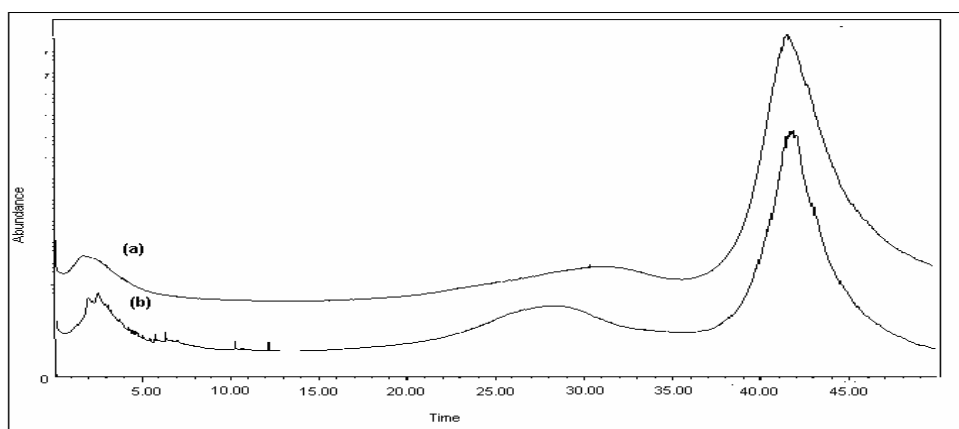
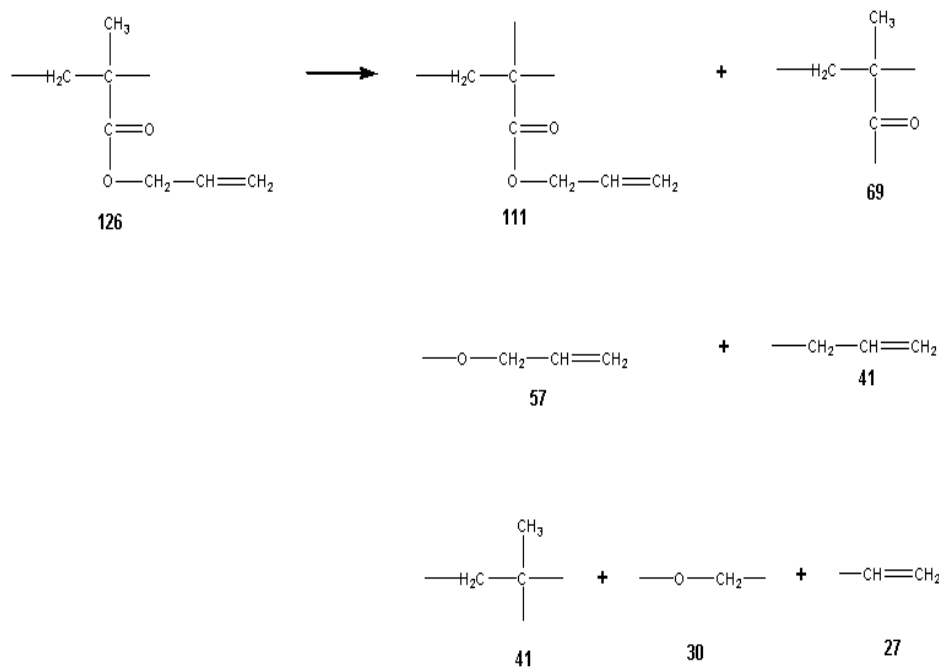
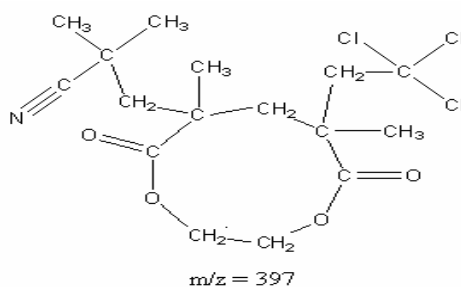


**Figure 3.19** Mass thermograms of (a) insoluble and (b) soluble PAMA fraction

The detailed fragmentation at 142, 335 and 442°C for insoluble PAMA fraction is given in Figures 3.20, 3.21, and 3.22, respectively. The relative abundances of the peaks and their fragments are given in Table 3.12. In Figure 3.20, the temperature is 142°C (11.7 min in Figure 3.19a). There is no apparent degradation peak at 11.7 min. Therefore, the peaks observed are due to the fragmentation of residual monomer and other possible oligomers that formed during the polymerization. The monomer peak at 126 is very weak in the spectrum showing the predominant monomer fragmentation. The residual monomer is degraded to give the main peaks at 27, 30, 41, 57, 69, and 111 (Table 3.12). The fragmentation of monomer is shown as follows:



The peak at 397 corresponds to a cyclic oligomer containing AIBN and CCl<sub>4</sub> fragments. The observed weak peaks at 398, 399 and 400 are due to same molecule with different Cl isotopes. The fragmentation of this product gives weak peaks at 377, 233, 203 and 171 (Table 3.12). The presence of Cl and N is also shown in the ESCA spectrum of PAMA.



The thermal fragmentation at 335°C is given in Figure 3.21 and results are tabulated in Table 3.12. The basic thermal behavior of polymer at the stage of degradation is mainly formation of anhydride and end group cyclization (Figure 3.8). Therefore, the anhydride formation and/or cyclization to lactones are shown in the degradation scheme.

The fragmentation at 442°C (Figure 3.22) for insoluble PAMA is similar to that at 335°C, with increasing number of fragments. These are mostly main chain degradation products.

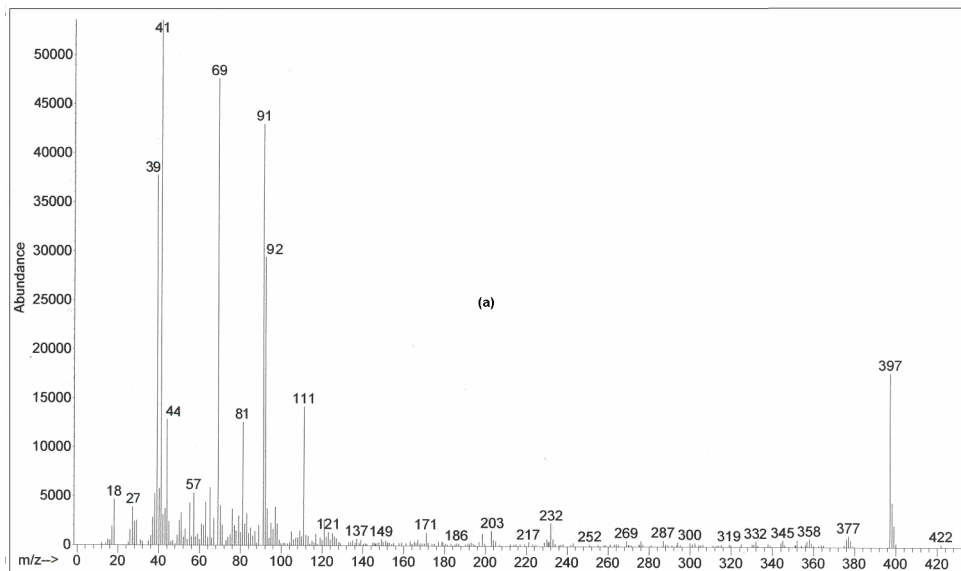


**Figure 3.20** Fragments from insoluble PAMA fraction obtained at 142°C

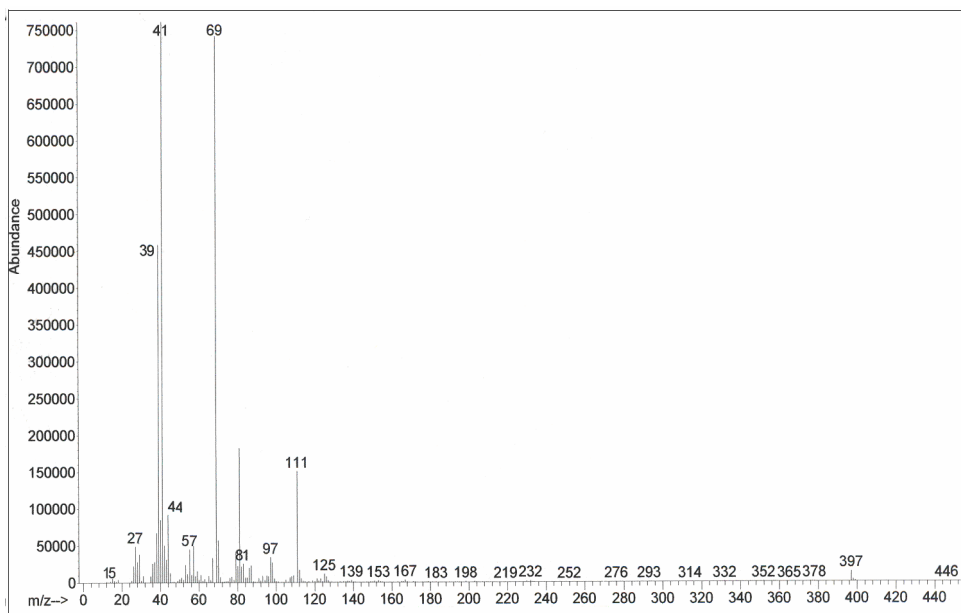


**Figure 3.21** Fragments from insoluble PAMA fraction obtained at 335°C

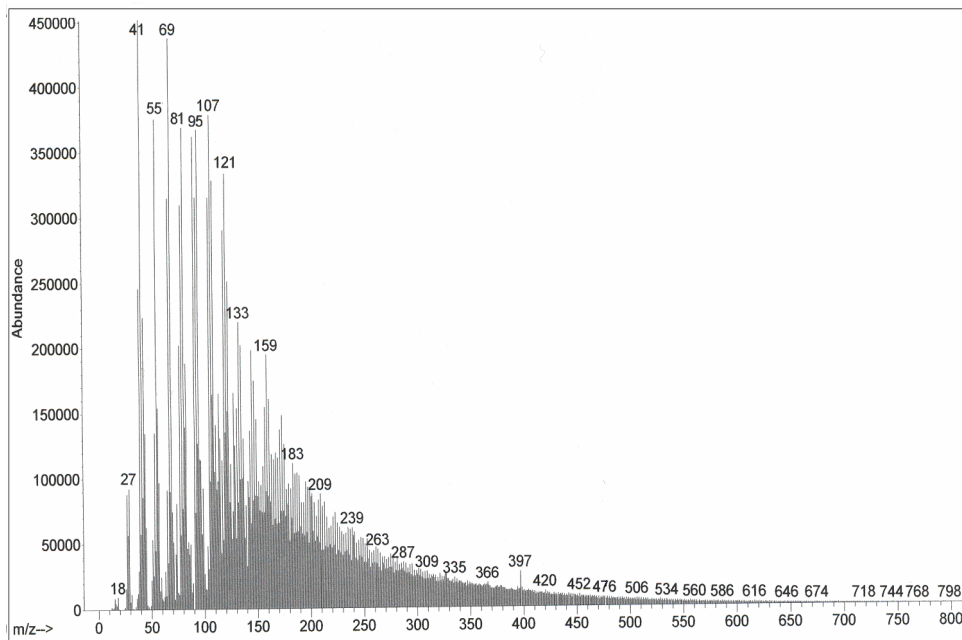


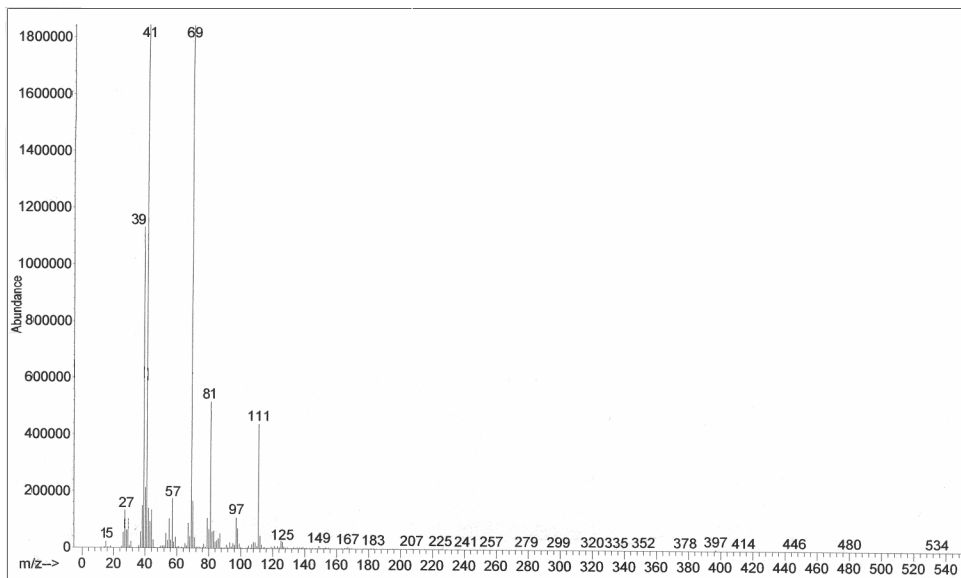
**Figure 3.22** Fragments from insoluble PAMA fraction obtained at 442°C

**Table 3.12** The relative abundances of the peaks and their fragments from insoluble PAMA fraction

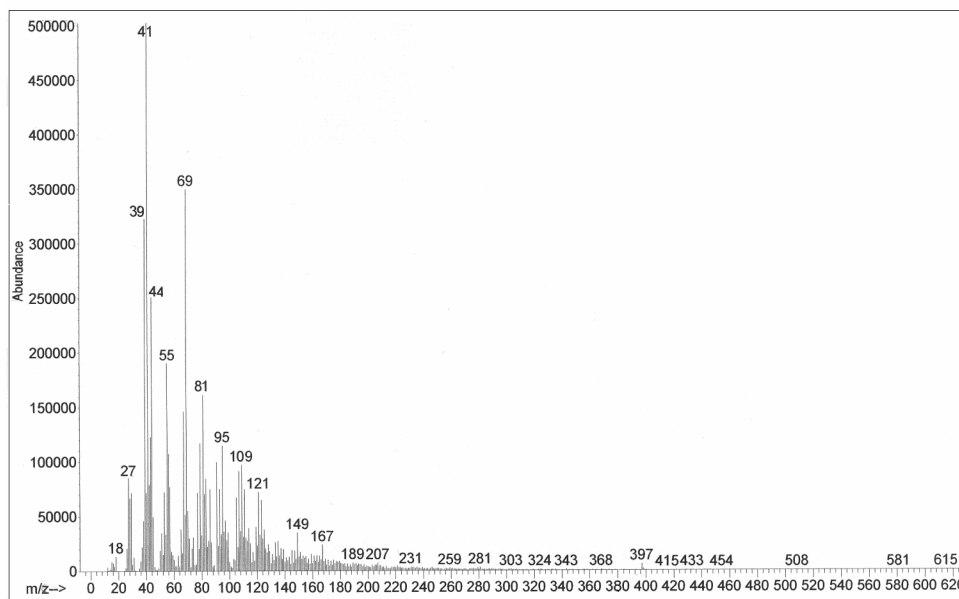
m/z	142°C		335°C		442°C	
	I/I <sub>0</sub>	fragments	I/I <sub>0</sub>	fragments	I/I <sub>0</sub>	fragments
15	0.11	CH <sub>3</sub>	1.05	CH <sub>3</sub>	1.05	CH <sub>3</sub>
18	0.65	H <sub>2</sub> O	0.57	H <sub>2</sub> O	1.12	H <sub>2</sub> O
26	0.24	CN, C <sub>2</sub> H <sub>2</sub>	2.93	CN, C <sub>2</sub> H <sub>2</sub>	2.15	CN, C <sub>2</sub> H <sub>2</sub>
27	0.49	C <sub>2</sub> H <sub>3</sub>	6.48	C <sub>2</sub> H <sub>3</sub>	11.64	C <sub>2</sub> H <sub>3</sub>
28	0.33	CO	3.70	CO	7.46	CO
31	0.08	CH <sub>3</sub> O	1.39	CH <sub>3</sub> O	1.46	CH <sub>3</sub> O
35	0.07	Cl	0.96	Cl	0.33	Cl
39	4.80	C <sub>3</sub> H <sub>3</sub>	60.26	C <sub>3</sub> H <sub>3</sub>	32.36	C <sub>3</sub> H <sub>3</sub>
41	7.07	C <sub>3</sub> H <sub>5</sub>	100	C <sub>3</sub> H <sub>5</sub>	58.43	C <sub>3</sub> H <sub>5</sub>
44	1.78	CO <sub>2</sub>	12.31	CO <sub>2</sub>	17.39	CO <sub>2</sub>
45	0.32	CHO <sub>2</sub>	1.77	CHO <sub>2</sub>	8.11	CHO <sub>2</sub>
55	0.56	C <sub>3</sub> H <sub>3</sub> O	6.21	C <sub>3</sub> H <sub>3</sub> O	48.86	C <sub>3</sub> H <sub>3</sub> O
57	0.70	C <sub>3</sub> H <sub>5</sub> O	7.69	C <sub>3</sub> H <sub>5</sub> O	12.74	C <sub>3</sub> H <sub>5</sub> O
69	6.14	C <sub>4</sub> H <sub>5</sub> O	97.79	C <sub>4</sub> H <sub>5</sub> O	56.46	C <sub>4</sub> H <sub>5</sub> O
77	0.30	C <sub>6</sub> H <sub>5</sub>	1.01	C <sub>6</sub> H <sub>5</sub>	26.19	C <sub>6</sub> H <sub>5</sub>
81	1.53	C <sub>4</sub> HO <sub>2</sub>	24.42	C <sub>4</sub> HO <sub>2</sub>	48.31	C <sub>4</sub> HO <sub>2</sub>
87	0.22	C <sub>4</sub> H <sub>7</sub> O <sub>2</sub>	2.76	C <sub>4</sub> H <sub>7</sub> O <sub>2</sub>	6.25	C <sub>4</sub> H <sub>7</sub> O <sub>2</sub>
91	5.84	C <sub>6</sub> H <sub>5</sub> N	0.87	C <sub>6</sub> H <sub>5</sub> N	47.72	C <sub>6</sub> H <sub>5</sub> N
95	0.25	C <sub>5</sub> H <sub>3</sub> O <sub>2</sub>	1.29	C <sub>5</sub> H <sub>3</sub> O <sub>2</sub>	48.08	C <sub>5</sub> H <sub>3</sub> O <sub>2</sub>
97	0.49	C <sub>5</sub> H <sub>5</sub> O <sub>2</sub>	4.61	C <sub>5</sub> H <sub>5</sub> O <sub>2</sub>	15.65	C <sub>5</sub> H <sub>5</sub> O <sub>2</sub>
107	0.06	C <sub>6</sub> H <sub>3</sub> O <sub>2</sub>	0.95	C <sub>6</sub> H <sub>3</sub> O <sub>2</sub>	48.82	C <sub>6</sub> H <sub>3</sub> O <sub>2</sub>
111	1.87	C <sub>6</sub> H <sub>7</sub> O <sub>2</sub>	19.94	C <sub>6</sub> H <sub>7</sub> O <sub>2</sub>	18.50	C <sub>6</sub> H <sub>7</sub> O <sub>2</sub>
117	0.15	CCl <sub>3</sub>	0.17	CCl <sub>3</sub>	15.21	CCl <sub>3</sub>
121	0.25	C <sub>7</sub> H <sub>5</sub> O <sub>2</sub>	0.71	C <sub>7</sub> H <sub>5</sub> O <sub>2</sub>	43.47	C <sub>7</sub> H <sub>5</sub> O <sub>2</sub>
123	0.17	C <sub>7</sub> H <sub>7</sub> O <sub>2</sub>	0.65	C <sub>7</sub> H <sub>7</sub> O <sub>2</sub>	33.40	C <sub>7</sub> H <sub>7</sub> O <sub>2</sub>
125	0.19	C <sub>7</sub> H <sub>9</sub> O <sub>2</sub>	1.49	C <sub>7</sub> H <sub>9</sub> O <sub>2</sub>	14.29	C <sub>7</sub> H <sub>9</sub> O <sub>2</sub>
126	0.10	C <sub>7</sub> H <sub>10</sub> O <sub>2</sub> (AMA)	1.09	C <sub>7</sub> H <sub>10</sub> O <sub>2</sub> (AMA)	6.87	C <sub>7</sub> H <sub>10</sub> O <sub>2</sub> (AMA)
133	0.04	C <sub>8</sub> H <sub>5</sub> O <sub>2</sub>	0.16	C <sub>8</sub> H <sub>5</sub> O <sub>2</sub>	28.70	C <sub>8</sub> H <sub>5</sub> O <sub>2</sub>
137	0.08	C <sub>6</sub> H <sub>5</sub> O <sub>3</sub>	0.22	C <sub>6</sub> H <sub>5</sub> O <sub>3</sub>	16.65	C <sub>6</sub> H <sub>5</sub> O <sub>3</sub>

Table 3.12 (continued)						
139	0.08	C <sub>6</sub> H <sub>7</sub> O <sub>3</sub>	0.41	C <sub>6</sub> H <sub>7</sub> O <sub>3</sub>	10.22	C <sub>6</sub> H <sub>7</sub> O <sub>3</sub>
149	0.12	C <sub>9</sub> H <sub>5</sub> O <sub>2</sub>	0.16	C <sub>9</sub> H <sub>5</sub> O <sub>2</sub>	19.59	C <sub>9</sub> H <sub>5</sub> O <sub>2</sub>
153	0.06	C <sub>9</sub> H <sub>9</sub> O <sub>2</sub>	0.32	C <sub>9</sub> H <sub>9</sub> O <sub>2</sub>	12.06	C <sub>9</sub> H <sub>9</sub> O <sub>2</sub>
159	0.04	C <sub>7</sub> H <sub>11</sub> O <sub>4</sub>	0.08	C <sub>7</sub> H <sub>11</sub> O <sub>4</sub>	25.63	C <sub>7</sub> H <sub>11</sub> O <sub>4</sub>
167	0.07	C <sub>8</sub> H <sub>7</sub> O <sub>4</sub>	0.06	C <sub>8</sub> H <sub>7</sub> O <sub>4</sub>	15.90	C <sub>8</sub> H <sub>7</sub> O <sub>4</sub>
171	0.22	C <sub>9</sub> H <sub>17</sub> O <sub>2</sub> N, C <sub>8</sub> H <sub>11</sub> O <sub>4</sub>	0.25	C <sub>9</sub> H <sub>17</sub> O <sub>2</sub> N, C <sub>8</sub> H <sub>11</sub> O <sub>4</sub>	18.41	C <sub>9</sub> H <sub>17</sub> O <sub>2</sub> N, C <sub>8</sub> H <sub>11</sub> O <sub>4</sub>
185	0.03	C <sub>9</sub> H <sub>13</sub> O <sub>4</sub>	0.05	C <sub>9</sub> H <sub>13</sub> O <sub>4</sub>	13.85	C <sub>9</sub> H <sub>13</sub> O <sub>4</sub>
195	-	C <sub>11</sub> H <sub>15</sub> O <sub>3</sub>	0.04	C <sub>11</sub> H <sub>15</sub> O <sub>3</sub>	12.45	C <sub>11</sub> H <sub>15</sub> O <sub>3</sub>
203	0.24	C <sub>12</sub> H <sub>13</sub> O <sub>2</sub> N	0.21	C <sub>12</sub> H <sub>13</sub> O <sub>2</sub> N	10.58	C <sub>12</sub> H <sub>13</sub> O <sub>2</sub> N
209	0.03	C <sub>11</sub> H <sub>13</sub> O <sub>4</sub>	0.04	C <sub>11</sub> H <sub>13</sub> O <sub>4</sub>	11.57	C <sub>11</sub> H <sub>13</sub> O <sub>4</sub>
219	0.03	C <sub>12</sub> H <sub>11</sub> O <sub>4</sub>	0.03	C <sub>12</sub> H <sub>11</sub> O <sub>4</sub>	8.43	C <sub>12</sub> H <sub>11</sub> O <sub>4</sub>
233	0.06	C <sub>14</sub> H <sub>19</sub> O <sub>2</sub> N, C <sub>14</sub> H <sub>16</sub> O <sub>4</sub>	0.07	C <sub>14</sub> H <sub>19</sub> O <sub>2</sub> N, C <sub>14</sub> H <sub>16</sub> O <sub>4</sub>	7.76	C <sub>14</sub> H <sub>19</sub> O <sub>2</sub> N, C <sub>14</sub> H <sub>16</sub> O <sub>4</sub>
252	0.02	C <sub>14</sub> H <sub>20</sub> O <sub>4</sub>	0.03	C <sub>14</sub> H <sub>19</sub> O <sub>4</sub>	6.96	C <sub>14</sub> H <sub>19</sub> O <sub>4</sub>
269	0.10	C <sub>14</sub> H <sub>21</sub> O <sub>5</sub>	0.09	C <sub>14</sub> H <sub>21</sub> O <sub>5</sub>	5.18	C <sub>14</sub> H <sub>21</sub> O <sub>5</sub>
276	0.09	C <sub>15</sub> H <sub>16</sub> O <sub>6</sub>	0.09	C <sub>15</sub> H <sub>16</sub> O <sub>6</sub>	4.16	C <sub>15</sub> H <sub>16</sub> O <sub>6</sub>
287	0.07	C <sub>14</sub> H <sub>23</sub> O <sub>6</sub>	0.07	C <sub>14</sub> H <sub>23</sub> O <sub>6</sub>	4.50	C <sub>14</sub> H <sub>23</sub> O <sub>6</sub>
293	0.03	C <sub>17</sub> H <sub>25</sub> O <sub>5</sub>	0.03	C <sub>17</sub> H <sub>25</sub> O <sub>5</sub>	4.33	C <sub>17</sub> H <sub>25</sub> O <sub>5</sub>
301	0.02	C <sub>15</sub> H <sub>25</sub> O <sub>6</sub>	0.05	C <sub>15</sub> H <sub>25</sub> O <sub>6</sub>	3.96	C <sub>15</sub> H <sub>25</sub> O <sub>6</sub>
319	0.05	C <sub>18</sub> H <sub>23</sub> O <sub>5</sub>	0.04	C <sub>18</sub> H <sub>23</sub> O <sub>5</sub>	3.02	C <sub>18</sub> H <sub>23</sub> O <sub>5</sub>
332	0.10	C <sub>18</sub> H <sub>20</sub> O <sub>6</sub>	0.10	C <sub>18</sub> H <sub>20</sub> O <sub>6</sub>	2.43	C <sub>18</sub> H <sub>20</sub> O <sub>6</sub>
345	0.08	C <sub>19</sub> H <sub>21</sub> O <sub>6</sub>	0.09	C <sub>19</sub> H <sub>21</sub> O <sub>6</sub>	2.44	C <sub>19</sub> H <sub>21</sub> O <sub>6</sub>
352	0.11	C <sub>19</sub> H <sub>28</sub> O <sub>6</sub>	0.09	C <sub>19</sub> H <sub>28</sub> O <sub>6</sub>	2.26	C <sub>19</sub> H <sub>28</sub> O <sub>6</sub>
358	0.07	C <sub>20</sub> H <sub>22</sub> O <sub>6</sub>	0.09	C <sub>20</sub> H <sub>22</sub> O <sub>6</sub>	2.22	C <sub>20</sub> H <sub>22</sub> O <sub>6</sub>
365	0.03	C <sub>20</sub> H <sub>29</sub> O <sub>6</sub>	0.03	C <sub>20</sub> H <sub>29</sub> O <sub>6</sub>	2.27	C <sub>20</sub> H <sub>29</sub> O <sub>6</sub>
377	0.13	C <sub>15</sub> H <sub>14</sub> Cl <sub>3</sub> O <sub>4</sub> N	0.10	C <sub>15</sub> H <sub>14</sub> Cl <sub>3</sub> O <sub>4</sub> N	2.07	C <sub>15</sub> H <sub>14</sub> Cl <sub>3</sub> O <sub>4</sub> N
378	0.10	C <sub>21</sub> H <sub>30</sub> O <sub>6</sub>	0.09	C <sub>21</sub> H <sub>30</sub> O <sub>6</sub>	2.04	C <sub>21</sub> H <sub>30</sub> O <sub>6</sub>
397	2.54	C <sub>16</sub> H <sub>22</sub> Cl <sub>3</sub> O <sub>4</sub> N	1.97	C <sub>16</sub> H <sub>22</sub> Cl <sub>3</sub> O <sub>4</sub> N	3.53	C <sub>16</sub> H <sub>22</sub> Cl <sub>3</sub> O <sub>4</sub> N
422	0.02	C <sub>22</sub> H <sub>30</sub> O <sub>8</sub>	-	C <sub>22</sub> H <sub>30</sub> O <sub>8</sub>	1.40	C <sub>22</sub> H <sub>30</sub> O <sub>8</sub>
616	-	C <sub>34</sub> H <sub>48</sub> O <sub>10</sub>	-	C <sub>34</sub> H <sub>48</sub> O <sub>10</sub>	0.25	C <sub>34</sub> H <sub>48</sub> O <sub>10</sub>
718	-	C <sub>40</sub> H <sub>46</sub> O <sub>12</sub>	-	C <sub>40</sub> H <sub>46</sub> O <sub>12</sub>	0.07	C <sub>40</sub> H <sub>46</sub> O <sub>12</sub>
798	-	C <sub>43</sub> H <sub>58</sub> O <sub>14</sub>	-	C <sub>43</sub> H <sub>58</sub> O <sub>14</sub>	0.04	C <sub>43</sub> H <sub>58</sub> O <sub>14</sub>

The mass spectrum for the soluble PAMA fraction is given in Figure 3.17b. The observed  $m/z$  at 309, 405, and 441°C are given in Figures 3.23, 3.24, and 3.25, respectively. The  $m/z$  data at three different temperatures are tabulated in Table 3.13. The fragment abundance is maximized at 335°C for the insoluble fraction of PAMA (Figure 3.21) and that of the soluble fraction is 309°C (Figure 3.23). The two thermograms are quite similar with changes in the relative abundance of fragments.



**Figure 3.23** Fragments from soluble PAMA fraction obtained at 309°C



**Figure 3.24** Fragments from soluble PAMA fraction obtained at 405°C

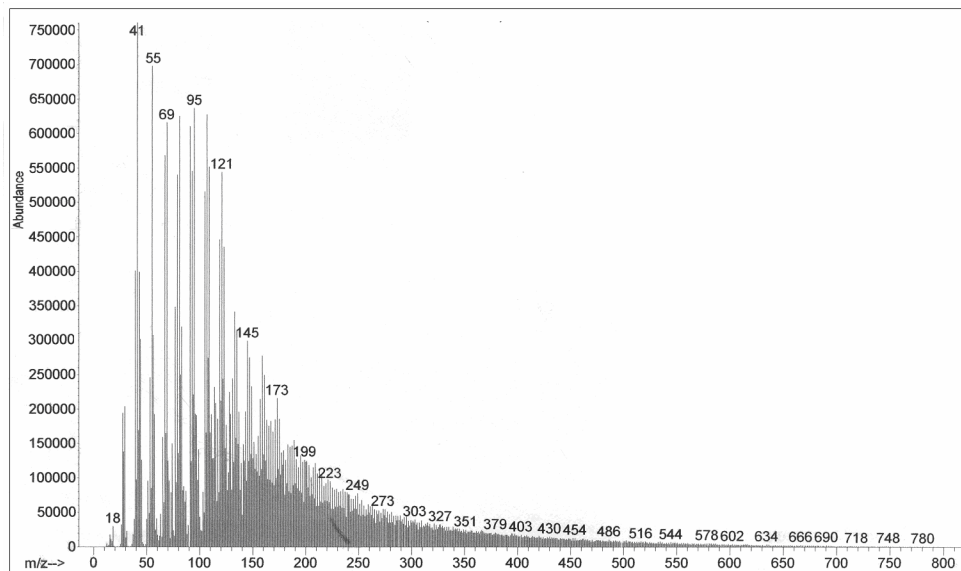


**Figure 3.25** Fragments from soluble PAMA fraction obtained at 441°C

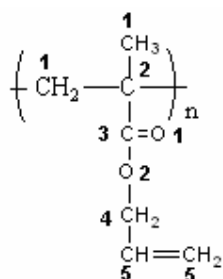
**Table 3.13** The relative abundances of the peaks and their fragments from soluble PAMA fraction

m/z	309°C		405°C		441°C	
	I/I <sub>0</sub>	fragments	I/I <sub>0</sub>	fragments	I/I <sub>0</sub>	fragments
15	1.21	CH <sub>3</sub>	0.57	CH <sub>3</sub>	0.98	CH <sub>3</sub>
18	0.33	H <sub>2</sub> O	0.72	H <sub>2</sub> O	1.68	H <sub>2</sub> O
26	2.97	CN, C <sub>2</sub> H <sub>2</sub>	1.17	CN, C <sub>2</sub> H <sub>2</sub>	1.61	CN, C <sub>2</sub> H <sub>2</sub>
27	6.94	C <sub>2</sub> H <sub>3</sub>	4.56	C <sub>2</sub> H <sub>3</sub>	10.25	C <sub>2</sub> H <sub>3</sub>
28	3.28	CO	3.77	CO	7.09	CO
29	5.46	C <sub>2</sub> H <sub>5</sub> , CHO	4.12	C <sub>2</sub> H <sub>5</sub> , CHO	10.97	C <sub>2</sub> H <sub>5</sub> , CHO
31	1.29	CH <sub>3</sub> O	0.59	CH <sub>3</sub> O	1.15	CH <sub>3</sub> O
35	0.10	Cl	0.13	Cl	0.04	Cl
39	60.63	C <sub>3</sub> H <sub>3</sub>	17.36	C <sub>3</sub> H <sub>3</sub>	21.48	C <sub>3</sub> H <sub>3</sub>
41	100	C <sub>3</sub> H <sub>5</sub>	27.25	C <sub>3</sub> H <sub>5</sub>	40.91	C <sub>3</sub> H <sub>5</sub>
44	6.93	CO <sub>2</sub>	13.78	CO <sub>2</sub>	15.84	CO <sub>2</sub>
45	1.45	CHO <sub>2</sub>	2.59	CHO <sub>2</sub>	6.56	CHO <sub>2</sub>
55	5.94	C <sub>3</sub> H <sub>3</sub> O	10.49	C <sub>3</sub> H <sub>3</sub> O	38.24	C <sub>3</sub> H <sub>3</sub> O
57	9.41	C <sub>3</sub> H <sub>5</sub> O	4.12	C <sub>3</sub> H <sub>5</sub> O	10.71	C <sub>3</sub> H <sub>5</sub> O
69	99.09	C <sub>4</sub> H <sub>5</sub> O	19.47	C <sub>4</sub> H <sub>5</sub> O	33.03	C <sub>4</sub> H <sub>5</sub> O
77	0.85	C <sub>6</sub> H <sub>5</sub>	3.53	C <sub>6</sub> H <sub>5</sub>	18.66	C <sub>6</sub> H <sub>5</sub>
81	27.22	C <sub>4</sub> HO <sub>2</sub>	8.78	C <sub>4</sub> HO <sub>2</sub>	33.65	C <sub>4</sub> HO <sub>2</sub>
87	3.14	C <sub>4</sub> H <sub>7</sub> O <sub>2</sub>	1.49	C <sub>4</sub> H <sub>7</sub> O <sub>2</sub>	4.32	C <sub>4</sub> H <sub>7</sub> O <sub>2</sub>
91	0.69	C <sub>6</sub> H <sub>5</sub> N	5.39	C <sub>6</sub> H <sub>5</sub> N	33.60	C <sub>6</sub> H <sub>5</sub> N
95	1.10	C <sub>5</sub> H <sub>3</sub> O <sub>2</sub>	6.10	C <sub>5</sub> H <sub>3</sub> O <sub>2</sub>	34.00	C <sub>5</sub> H <sub>3</sub> O <sub>2</sub>
97	5.62	C <sub>5</sub> H <sub>5</sub> O <sub>2</sub>	2.54	C <sub>5</sub> H <sub>5</sub> O <sub>2</sub>	10.67	C <sub>5</sub> H <sub>5</sub> O <sub>2</sub>
107	0.82	C <sub>6</sub> H <sub>3</sub> O <sub>2</sub>	5.13	C <sub>6</sub> H <sub>3</sub> O <sub>2</sub>	34.28	C <sub>6</sub> H <sub>3</sub> O <sub>2</sub>
111	23.35	C <sub>6</sub> H <sub>7</sub> O <sub>2</sub>	4.00	C <sub>6</sub> H <sub>7</sub> O <sub>2</sub>	10.36	C <sub>6</sub> H <sub>7</sub> O <sub>2</sub>
117	0.19	CCl <sub>3</sub>	1.07	CCl <sub>3</sub>	10.26	CCl <sub>3</sub>
121	0.52	C <sub>7</sub> H <sub>5</sub> O <sub>2</sub>	3.75	C <sub>7</sub> H <sub>5</sub> O <sub>2</sub>	29.92	C <sub>7</sub> H <sub>5</sub> O <sub>2</sub>
123	0.50	C <sub>7</sub> H <sub>7</sub> O <sub>2</sub>	3.50	C <sub>7</sub> H <sub>7</sub> O <sub>2</sub>	23.58	C <sub>7</sub> H <sub>7</sub> O <sub>2</sub>
125	1.66	C <sub>7</sub> H <sub>9</sub> O <sub>2</sub>	1.95	C <sub>7</sub> H <sub>9</sub> O <sub>2</sub>	9.17	C <sub>7</sub> H <sub>9</sub> O <sub>2</sub>
126	1.15	C <sub>7</sub> H <sub>10</sub> O <sub>2</sub> (AMA)	1.18	C <sub>7</sub> H <sub>10</sub> O <sub>2</sub> (AMA)	4.38	C <sub>7</sub> H <sub>10</sub> O <sub>2</sub> (AMA)
133	0.30	C <sub>8</sub> H <sub>5</sub> O <sub>2</sub>	1.41	C <sub>8</sub> H <sub>5</sub> O <sub>2</sub>	18.31	C <sub>8</sub> H <sub>5</sub> O <sub>2</sub>

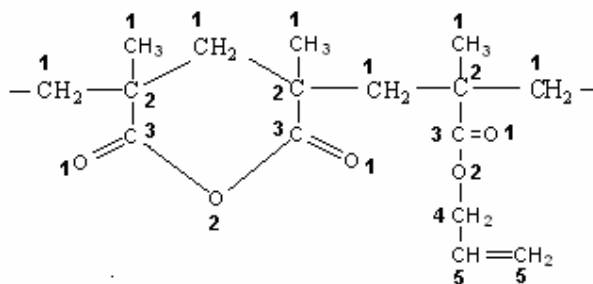
137	0.29	C <sub>6</sub> H <sub>5</sub> O <sub>3</sub>	1.07	C <sub>6</sub> H <sub>5</sub> O <sub>3</sub>	10.66	C <sub>6</sub> H <sub>5</sub> O <sub>3</sub>
139	0.28	C <sub>6</sub> H <sub>7</sub> O <sub>3</sub>	1.05	C <sub>6</sub> H <sub>7</sub> O <sub>3</sub>	6.67	C <sub>6</sub> H <sub>7</sub> O <sub>3</sub>
149	0.62	C <sub>9</sub> H <sub>5</sub> O <sub>2</sub>	1.71	C <sub>9</sub> H <sub>5</sub> O <sub>2</sub>	12.62	C <sub>9</sub> H <sub>5</sub> O <sub>2</sub>
153	0.21	C <sub>9</sub> H <sub>9</sub> O <sub>2</sub>	0.75	C <sub>9</sub> H <sub>9</sub> O <sub>2</sub>	7.34	C <sub>9</sub> H <sub>9</sub> O <sub>2</sub>
159	0.06	C <sub>7</sub> H <sub>11</sub> O <sub>4</sub>	0.76	C <sub>7</sub> H <sub>11</sub> O <sub>4</sub>	15.64	C <sub>7</sub> H <sub>11</sub> O <sub>4</sub>
167	0.31	C <sub>8</sub> H <sub>7</sub> O <sub>4</sub>	1.42	C <sub>8</sub> H <sub>7</sub> O <sub>4</sub>	10.20	C <sub>8</sub> H <sub>7</sub> O <sub>4</sub>
171	0.11	C <sub>9</sub> H <sub>17</sub> O <sub>2</sub> N, C <sub>8</sub> H <sub>11</sub> O <sub>4</sub>	0.46	C <sub>9</sub> H <sub>17</sub> O <sub>2</sub> N, C <sub>8</sub> H <sub>11</sub> O <sub>4</sub>	10.27	C <sub>9</sub> H <sub>17</sub> O <sub>2</sub> N, C <sub>8</sub> H <sub>11</sub> O <sub>4</sub>
185	0.16	C <sub>9</sub> H <sub>13</sub> O <sub>4</sub>	0.39	C <sub>9</sub> H <sub>13</sub> O <sub>4</sub>	7.85	C <sub>9</sub> H <sub>13</sub> O <sub>4</sub>
195	0.11	C <sub>11</sub> H <sub>15</sub> O <sub>3</sub>	0.40	C <sub>11</sub> H <sub>15</sub> O <sub>3</sub>	7.44	C <sub>11</sub> H <sub>15</sub> O <sub>3</sub>
203	0.06	C <sub>12</sub> H <sub>13</sub> O <sub>2</sub> N	0.35	C <sub>12</sub> H <sub>13</sub> O <sub>2</sub> N	6.71	C <sub>12</sub> H <sub>13</sub> O <sub>2</sub> N
209	0.09	C <sub>11</sub> H <sub>13</sub> O <sub>4</sub>	0.29	C <sub>11</sub> H <sub>13</sub> O <sub>4</sub>	6.78	C <sub>11</sub> H <sub>13</sub> O <sub>4</sub>
219	0.03	C <sub>12</sub> H <sub>11</sub> O <sub>4</sub>	0.23	C <sub>12</sub> H <sub>11</sub> O <sub>4</sub>	5.29	C <sub>12</sub> H <sub>11</sub> O <sub>4</sub>
233	0.05	C <sub>14</sub> H <sub>19</sub> O <sub>2</sub> N, C <sub>14</sub> H <sub>16</sub> O <sub>4</sub>	0.15	C <sub>14</sub> H <sub>19</sub> O <sub>2</sub> N, C <sub>14</sub> H <sub>16</sub> O <sub>4</sub>	4.40	C <sub>14</sub> H <sub>19</sub> O <sub>2</sub> N, C <sub>14</sub> H <sub>16</sub> O <sub>4</sub>
252	0.04	C <sub>14</sub> H <sub>20</sub> O <sub>4</sub> (dimer)	0.09	C <sub>14</sub> H <sub>19</sub> O <sub>4</sub> (dimer)	2.57	C <sub>14</sub> H <sub>19</sub> O <sub>4</sub> (dimer)
269	0.03	C <sub>14</sub> H <sub>21</sub> O <sub>5</sub>	0.07	C <sub>14</sub> H <sub>21</sub> O <sub>5</sub>	3.15	C <sub>14</sub> H <sub>21</sub> O <sub>5</sub>
287	0.04	C <sub>14</sub> H <sub>23</sub> O <sub>6</sub>	0.05	C <sub>14</sub> H <sub>23</sub> O <sub>6</sub>	2.60	C <sub>14</sub> H <sub>23</sub> O <sub>6</sub>
301	0.02	C <sub>15</sub> H <sub>25</sub> O <sub>6</sub>	0.04	C <sub>15</sub> H <sub>25</sub> O <sub>6</sub>	2.24	C <sub>15</sub> H <sub>25</sub> O <sub>6</sub>
319	0.01	C <sub>18</sub> H <sub>23</sub> O <sub>5</sub>	0.06	C <sub>18</sub> H <sub>23</sub> O <sub>5</sub>	1.75	C <sub>18</sub> H <sub>23</sub> O <sub>5</sub>
332	0.04	C <sub>18</sub> H <sub>20</sub> O <sub>6</sub>	0.06	C <sub>18</sub> H <sub>20</sub> O <sub>6</sub>	1.39	C <sub>18</sub> H <sub>20</sub> O <sub>6</sub>
345	0.02	C <sub>19</sub> H <sub>21</sub> O <sub>6</sub>	0.04	C <sub>19</sub> H <sub>21</sub> O <sub>6</sub>	1.39	C <sub>19</sub> H <sub>21</sub> O <sub>6</sub>
352	0.04	C <sub>19</sub> H <sub>28</sub> O <sub>6</sub>	0.02	C <sub>19</sub> H <sub>28</sub> O <sub>6</sub>	1.15	C <sub>19</sub> H <sub>28</sub> O <sub>6</sub>
358	0.01	C <sub>20</sub> H <sub>22</sub> O <sub>6</sub>	0.03	C <sub>20</sub> H <sub>22</sub> O <sub>6</sub>	1.24	C <sub>20</sub> H <sub>22</sub> O <sub>6</sub>
365	0.02	C <sub>20</sub> H <sub>29</sub> O <sub>6</sub>	0.03	C <sub>20</sub> H <sub>29</sub> O <sub>6</sub>	1.26	C <sub>20</sub> H <sub>29</sub> O <sub>6</sub>
378	0.01	C <sub>21</sub> H <sub>30</sub> O <sub>6</sub> (trimer)	0.02	C <sub>21</sub> H <sub>30</sub> O <sub>6</sub> (trimer)	1.11	C <sub>21</sub> H <sub>30</sub> O <sub>6</sub> (trimer)
397	0.26	C <sub>16</sub> H <sub>22</sub> Cl <sub>3</sub> O <sub>4</sub> N	0.24	C <sub>16</sub> H <sub>22</sub> Cl <sub>3</sub> O <sub>4</sub> N	1.08	C <sub>16</sub> H <sub>22</sub> Cl <sub>3</sub> O <sub>4</sub> N
422	-	C <sub>22</sub> H <sub>30</sub> O <sub>8</sub>	-	C <sub>22</sub> H <sub>30</sub> O <sub>8</sub>	0.98	C <sub>22</sub> H <sub>30</sub> O <sub>8</sub>
624	-	C <sub>35</sub> H <sub>44</sub> O <sub>10</sub>	0.01	C <sub>35</sub> H <sub>44</sub> O <sub>10</sub>	0.04	C <sub>35</sub> H <sub>44</sub> O <sub>10</sub>
748	-	C <sub>42</sub> H <sub>52</sub> O <sub>12</sub>	-	C <sub>42</sub> H <sub>52</sub> O <sub>12</sub>	0.04	C <sub>42</sub> H <sub>52</sub> O <sub>12</sub>
800	-	C <sub>43</sub> H <sub>60</sub> O <sub>14</sub>	-	C <sub>43</sub> H <sub>60</sub> O <sub>14</sub>	0.01	C <sub>43</sub> H <sub>60</sub> O <sub>14</sub>

### 3.2.6. XPS Investigation

In order to verify the presence of initiator and solvent fragments in the polymer, the detailed surface analysis of PAMA before and after pyrolysis at 350°C were done by XPS, and given in Figures 3.26a and b, respectively. The PAMA gives high amounts of anhydride at around 350°C. Therefore, the XPS results should be in agreement with other methods discussed above. The peak fitting was done by SpecLab program and the data are given in Table 3.14 based on the assigned atomic numbers in molecular formulas below.



(before thermal treatment)



(after thermal treatment)

**Table 3.14** The assignment of atomic eV to XPS peaks for PAMA

Poly(allyl methacrylate)						
	1	2	3	4	5	Atomic %
C 1s (eV)	285.00	285.82	288.94	287.19	284.45	77.3
O 1s (eV)	531.93	533.39				21.2
N 1s (eV)	398.37					1.1
Cl 2p (eV)	200.14					0.4
Poly(allyl methacrylate)-thermally treated at 350°C						
	1	2	3	4	5	Atomic %
C 1s (eV)	285.00	285.77	288.27	287.14	284.35	75.9
O 1s (eV)	532.08	533.49				21.3
N 1s (eV)	399.07					2.8

The fragments of initiator and solvent observed in spectroscopic measurements were also found from XPS. The atomic percent of N 1s was 1.1 in PAMA and increased to 2.8 after thermal treatment at 350°C. The degradation at 350°C is a linkage type with the evolution of pendant allyl group fragments. Therefore, the atomic percent of C and O are decreased and this causes an overall increase in percent for the N. This was also observed in NMR and FT-IR spectra. The atomic percent of Cl 2p was 0.4 before and not observed (resolution power of 0.1 atomic %) after thermal treatment. Loosely bonded Cl is removed by volatilization with thermal treatment with a decrease in concentration below the resolution power of XPS. Similar results were observed in Figure 3.8, where the intensity of C-Cl peak at 752 cm<sup>-1</sup> decreased with increase of temperature to 350°C. The atomic percentage (Table 3.14) in polymer chain is in agreement with calculated values. The peak fitting of PAMA for C 1s and O 1s are given in Figures 3.27a and b, respectively. The peak fitting for C 1s and for O 1s showed the expected binding energy

values of C<sub>1</sub>.....C<sub>5</sub> and O<sub>1</sub>, O<sub>2</sub>. After thermal treatment, the changes in positions and percentages are in agreement with the anhydride formation as shown in the degradation scheme. The presence of allyl group (-CH=CH<sub>2</sub>) at 284.45 eV with the percent atomic abundance shows that allyl groups are retained during the polymerization. However, after thermal treatment the percent atomic abundance decreased in accordance. Thus, XPS analysis gives no data for the lactones formation which is in agreement with the other experimental findings.

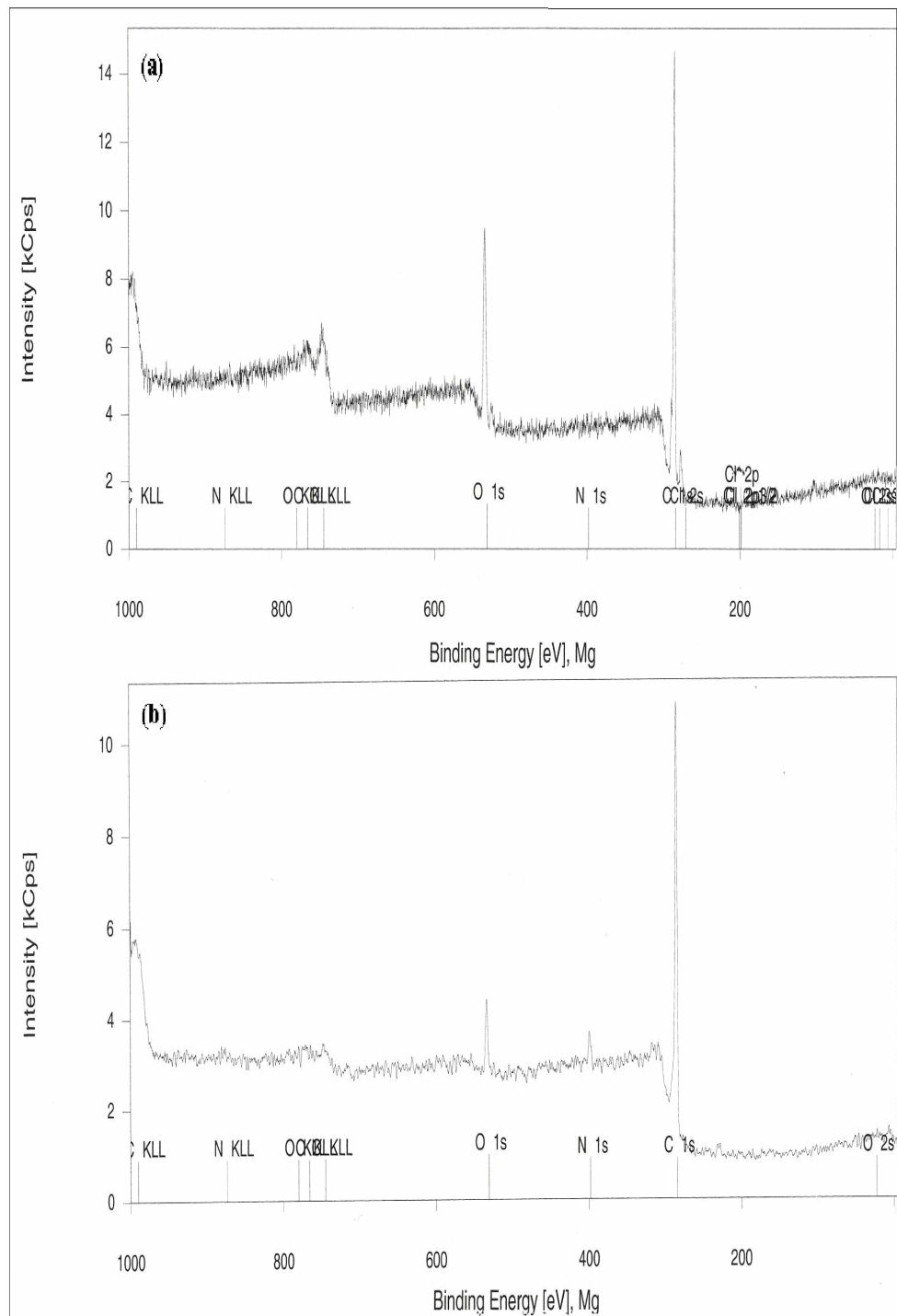


**Figure 3.26** XPS spectra of PAMA (a) before, (b) after pyrolysis at 350°C

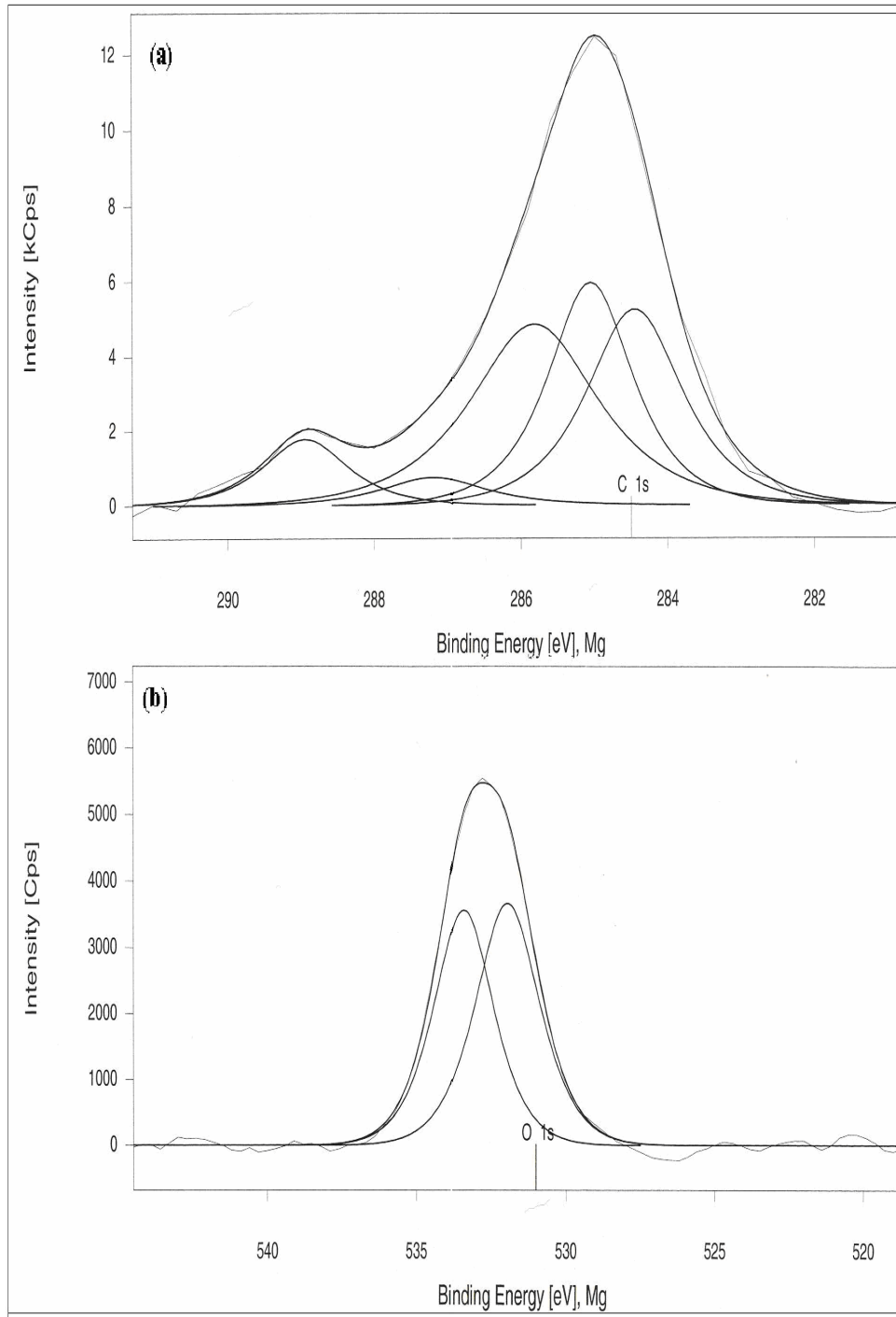


**Figure 3.27** XPS spectra of peak fitting of (a) C 1s and (b) O 1s of PAMA

### 3.2.7. DLS Investigation

The polymer obtained is insoluble in common organic solvent. Therefore, the measurement of the molecular weight was not possible. However, to get an idea about the relationship between molecular weight and the solubility property of the polymer, molecular weight for soluble fraction of PAMA was investigated by dynamic light scattering method. The calculated refractive index increment from refractive indexes measured in toluene solution of PAMA at 25°C was 0.0275 ml/g. The molecular weights measured for 3 samples are given in Table 3.15. The molecular weight for the first sample is  $2.7 \times 10^4$ . Therefore, even at this high molecular weight, polymer is soluble. The insoluble fractions will have molecular weight much larger than these values. The radius of gyration,  $R_g$  and end-to-end distance,  $\langle S^2 \rangle$  increased with molecular weight. Since it was shown by other experimental data that crosslinking or cyclopolymerization via allyl groups has not taken place, the insolubility of polymer can only be explained by molecular weight higher than the measured values. For some samples, the molecular weight measurements did not give reproducible results due to the insolubility of the samples.

**Table 3.15** DLS results for soluble fraction of PAMA.

Sample	$\overline{MW} \times 10^4$	$A_2 \times 10^{-7} \text{ (mol.dm/g}^2\text{)}$	$\langle S^2 \rangle \times 10^{-4} \text{ (}\mu\text{m}^2\text{)}$	$R_g \text{ (nm)}$
1	2.712	-2.901	5.751	23.981
2	112.0	3.379	9.279	30.461
3	132.1	0.9397	13.96	37.366

### 3.2.8. Powder XRD Investigation

The structural information was investigated by XRD. The XRD diffraction patterns of PAMA, cured at 125 and 175 °C are shown in Figures 3.28a, b and c, respectively. The powder pattern showed that PAMA is generally amorphous but there are certain regular orientations and also some crystallinity appearing as small peaks on the curve. These are scale extended in Figure 3.28d. When the sample is cured, some of the crystallinity peaks disappeared and the main peak showing orientations overlapped with a broad peak which is typical for a network polymer.

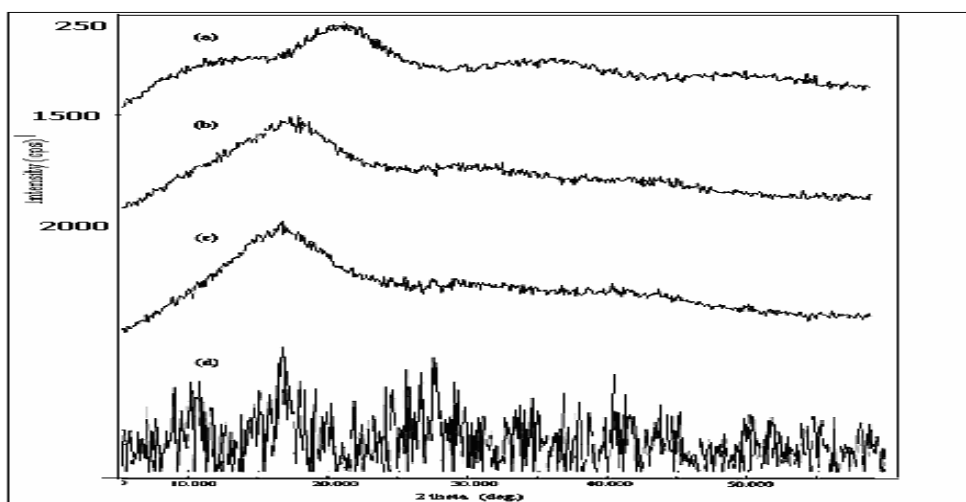


**Figure 3.28** XRD patterns of (a) PAMA with 62% conversion, (b) same PAMA cured at 125°C, (c) cured at 175°C , and (d) extended form of (c)

## CHAPTER 4

### 4. CONCLUSION

From the results of these experimental investigations, the following conclusions can be made:

- 1.** The FT-IR and NMR investigations showed that polymerization of AMA takes place through vinyl carbon-carbon double bond.
- 2.** The FT-IR and NMR investigations showed that there are no considerable amounts of lactones and anhydride formation during the polymerization.
- 3.** The NMR investigation showed clearly that even in very high conversions most of the allyl groups were retained as pendant groups and about 1-2% involved in crosslinking and/or cyclization.
- 4.** The DLS investigation showed that even for the soluble fractions, the molecular weight of polymer obtained was about  $1.1 \times 10^6$ . Therefore, for the insoluble fractions the molecular weight would be much higher.

- 5.** The DSC investigations showed that after annealing T<sub>g</sub> increased from 94 to 211°C.
- 6.** The TGA and MS degradation results in anhydride formation. It also showed that degradation of the PAMA chain is generally a depolymerization type.
- 7.** In literature, the insolubility of the polymer is attributed to the crosslinking by allyl group and/or cyclopolymerization. However, it was shown in this work that the main reason of insolubility is due to the high molecular weight of polymer.
- 8.** PAMA can be extensively used as a biomaterial when polymerized under suitable conditions to obtain linear polymer with controlled molecular weight. The curing after desired application for the proper use will give thermosetting material.

## REFERENCES

1. Blout, E.R.; Ostberg, B.E., *J. Polym. Sci.* 1946, 1, 230
2. D'alelio, G. F.; Hoffend, T. R., *J. Polym. Sci.: Part A-1* 1967, 5, 323-337.
3. Zhang, H.; Ruckenstein, E., *J. Polym. Sci.: Part A: Polym. Chem.* 1997, 35, 2901-2906.
4. Cohen, S.G.; Sparrow, D. B., *J. Polym. Sci.* 1948, 3, 693-703.
5. Higgins, J. P. J.; Weale, K. E., *J. Polym. Sci.: Part A-1* 1968, 6, 3007-3013.
6. Matsumoto, A.; Ishido, H.; Oiwa, M., *J. Polym. Sci.: Polym. Chem. Ed.* 1982, 20, 3207-3217.
7. Heatley, F.; Lovell, P. A.; Mc Donald, J., *Eur. Polym. J.* 1993, 29, 255-268.
8. Matsumoto, A.; Asai, S.; Aota, H., *Macromol. Chem. Phys.* 2000, 201, 2735-2741.
9. Matsumoto, A.; Asai, S.; Shimizu, S.; Aota, H., *Eur. Polym. J.* 2002, 38, 863-868.
10. Matsumoto, A.; Fujihashi, M.; Aota, H., *Eur. Polym. J.* 2003, 39, 2023-2027.
11. Paris, R.; de la Fuente, J. L., *J. Polym. Sci.: Part A: Polym. Chem.* 2004, 43, 2395-2406.
12. Hirano, T.; Kitayama, T.; Cao, J.; Hatada, K. *Polym. J.* 2000, 32, 961-969

- 13.** Mennicken, M.; Nagelsdiek, R.; Keul, H.; Höcker, H., *Macromol. Chem. Phys.* 2004, 205, 2429-2437.
- 14.** Nagelsdiek, R.; Mennicken, M.; Maier, B.; Keul, H.; Höcker, H., *Macromolecules* 2004, 37, 8923-8932.
- 15.** Liu, Y.; Mao, R.; Huglin, M. B., *Polymer* 1996, 37, 1437-1441.
- 16.** Cohen, S. G.; Ostberg, B. E.; Sparrow, D. B; Blout, E. R., *J. Polym. Sci.* 1948, 3, 264-282.
- 17.** Matsumoto, A., *Macromol. Symp.* 2002, 179, 141-152.
- 18.** Zulfigar, S., Masud, K., Piracha, A., and McNeill, I.C, (1997) *Polym. Degrad. Stab.*, 55: 257 - 263.
- 19.** Zulfigar, S., Piracha, A., and Masud, K. (1996) *Polym. Degrad. Stab.*, 52: 89 - 93.
- 20.** Zulfigar, S. and Masud, K. (2002) *Polym. Degrad. Stab.*, 78: 305 - 313.